

**ENHANCED EVAPORATIVE FLUX  
TO REMEDIATE SOILS  
CONTAMINATED WITH  
PRODUCED WATER BRINE**

by

Kathryn L. Platt

A thesis submitted to the Faculty of the University of Delaware in partial fulfillment of the requirements for the degree of Master of Civil Engineering

Summer 2020

© 2020 Kathryn L. Platt  
All Rights Reserved

**ENHANCED EVAPORATIVE FLUX  
TO REMEDIATE SOILS  
CONTAMINATED WITH  
PRODUCED WATER BRINE**

by

Kathryn L. Platt

Approved: \_\_\_\_\_  
Dominic M. Di Toro, Ph.D.  
Professor in charge of thesis on behalf of the Advisory Committee

Approved: \_\_\_\_\_  
Paul Imhoff, Ph.D.  
Professor in charge of thesis on behalf of the Advisory Committee

Approved: \_\_\_\_\_  
Jack Puleo, Ph.D.  
Chair of the Department of Civil and Environmental Engineering

Approved: \_\_\_\_\_  
Levi Thompson, Ph.D.  
Dean of the College of Engineering

Approved: \_\_\_\_\_  
Douglas J. Doren, Ph.D.  
Interim Vice Provost for Graduate and Professional Education and  
Dean of the Graduate College

## ACKNOWLEDGMENTS

First, I would like to thank ExxonMobil for providing financial support for this project. Specifically, thanks to Dr. Thomas Parkerton for approaching our team with his idea for this research and for trusting us to explore it. Without his vision, I would not have had this wonderful opportunity to learn. Thanks to everyone who joined our Zoom meetings and any who played a role in obtaining real produced water samples.

Secondly, I extend a huge thank you to my four mentors: Dr. Dominic Di Toro and Dr. Paul Imhoff at the University of Delaware, as well as Dr. Richard Carbonaro and Dr. Herbert Allen. They say it takes a village. Thanks for always being brains to pick and providing constant wisdom and insights. Your guidance provided not only direction in this project, but also direction in my life. Listening to your suggestions has shaped me into a better researcher and provided me with numerous tools to take with me as I venture on to my PhD. I aspire to attain the amount of curiosity and knowledge that each of you have collected.

A big thank you to Nikki Bugher for spending multiple semesters in the lab helping with the project. Nikki played a pivotal role in completing the USGS database analysis and spectrophotometry work, among other tasks. Your drive to accomplish and eagerness to learn are inspiring and helped reignite my passion for the project.

To everyone else at UD, including my fellow graduate students, professors, safety managers, and academic advisors, thanks for creating an environment that made my experience as a graduate student so incredibly enjoyable.

Lastly, I would of course like to thank my family, boyfriend, and friends for their constant support and inquiries asking, “how are the salts growing?” Thanks for always listening to my practice presentations and proof-reading my writing and providing endless fun outside of school. What a wonderful support team I have.

Cheers to everyone! On to the next adventure to keep on growing!

## TABLE OF CONTENTS

LIST OF TABLES .....	vi
LIST OF FIGURES .....	vii
ABSTRACT .....	ix

### Chapter

1 INTRODUCTION .....	1
2 MATERIALS & METHODS .....	5
1.1 Produced Waters and Crystallization Modifiers.....	5
1.2 Experiments Evaluating PHREEQC Model.....	7
1.3 Sand Experiments .....	8
1.4 Spectrophotometric Analysis of Ferrocyanide Fate .....	10
1.5 Solution Evaporation Experiments.....	11
1.6 PHREEQC Modeling .....	11
3 RESULTS.....	13
2.1 Evaluation of PHREEQC Model.....	13
2.2 Sand Experiments .....	16
2.2.1 Comparing Ferrocyanide Forms.....	16
2.2.2 Prussian Yellow Sand Columns .....	19
2.3 Spectrophotometric Analysis of Ferrocyanide Fate .....	21
2.4 Solution Evaporation Experiments.....	23
2.5 EDTA Sand Column Experiments .....	25
2.6 PHREEQC Modeling .....	27
4 DISCUSSIONS & CONCLUSIONS .....	30
REFERENCES .....	32

### Appendix

A SUPPORTING INFORMATION .....	34
B SUMMARY OF YEAR 1 WORK WITH BARITE .....	38

## LIST OF TABLES

Table A1: Produced Water Compositions (mg/L).....	34
Table A2: Produced Water Comparisons to USGS Database .....	34
Table A3: pHs of Some Solutions used in Sand Column Trials .....	35

## LIST OF FIGURES

- Figure 1: (A) Schematic of the soil profile at a brine-contaminated site showing water and salt concentration gradients. (B) Salts are expected to move upwards within the soil along with the advection of water. (C) Clogging of soil pores without inhibitor vs. (D) efflorescence on the soil surface with inhibitor. .... 2
- Figure 2: Comparison of  $\text{Ca}^{+2}$ ,  $\text{Cl}^-$ , and  $\text{Na}^+$  concentrations found in produced waters in various basins across the United States. .... 7
- Figure 3: PHREEQC modeling of changes in the salt saturation indices and precipitate salt volumes ( $\text{cm}^3$  of salt per liter of brine) with increasing evaporation. A) Delaware SI, B) Midland SI, C) Delaware volumes, D) Midland volumes. Followed by the experimental results of electroconductivity changes during evaporation in the E) Delaware and F) Midland. .... 15
- Figure 4: Top view of sand column beakers without any modifier (0 mM) and with varying forms of ferrocyanide (Prussian yellow, Prussian Blue, and Prussian Blue +  $\text{NH}_4\text{OH}$ ) at 1 and 10 mM concentrations. Images taken after 21 days of evaporation. .... 17
- Figure 5: The effects of Prussian yellow (PY), Prussian Blue (PB), and Prussian Blue + 0.033 M  $\text{NH}_4\text{OH}$  on salt column efflorescence. All three brines, 3.8 M NaCl, Delaware PW, and Midland PW were tested at 0, 1, and 10 mM ferrocyanide concentrations An \* signifies a beaker that produced crystallization on the surface, but formed a hard crust that was impossible to separate from the sand column. .... 18
- Figure 6: Sand column photos for the beakers with 1mM and 10 mM Prussian yellow additions. Top row gives top view of beakers while bottom provide profile views. Columns 1+2) 3.8 M NaCl, 3+4) Delaware PW, 5+6) Midland PW ..... 19
- Figure 7: Surface salt efflorescence of sand columns with varying concentrations of Prussian yellow for NaCl, Delaware PW and Midland PW..... 21
- Figure 8: Spectrophotometry results for fraction of Prussian yellow removed with effloresced salts versus fraction of salt effloresced. .... 22

Figure 9: Camera (circles) and SEM (rectangles) images of salts formed in beakers of 30mL of 3.8M NaCl, Delaware, or Midland produced waters. Showing effects of adding 0, 1, or 10 mM Prussian yellow. ....	24
Figure 10: Surface salt efflorescence of sand columns with varying concentrations of EDTA. Data shown for columns with 3.8 M NaCl, Delaware PW, and Midland PW. All columns had 1 mM Prussian yellow. ....	25
Figure 11: Surface salt efflorescence of beakers with varying amount of EDTA that were pH adjusted to neutral pH. Data shown for the Delaware and Midland PWs. All with 1 mM Prussian yellow.....	27
Figure 12: PHREEQC modeling of the speciation of 1mM ferrocyanide in the Delaware PW (left) and Midland PW (right). The speciation of the ferrocyanide ion is tracked as it creates complexes with Ba, Ca, H, K, Mg, and Na as EDTA is titrated into the solution as a chelating agent...	28
Figure A1: Calibration curves for electroconductivity of brines and corresponding molarities. ....	36
Figure A2: Calibration curve for Prussian yellow concentration and corresponding absorbances. ....	36
Figure A3: Efficiency of using spectrophotometry to measure Prussian yellow presence in the beakers. Y-axis values are the moles of Prussian yellow added to solution at the beginning of the experiment. X-axis values are the total moles of Prussian yellow found in the surface-scraped salt and remaining sand column after evaporation. X-axis values were determined using spectrophotometry and the calibration curve found in Figure A2. ....	37

## **ABSTRACT**

Hydraulic fracturing rates have shown significant growth in the past few years and this trend is expected to continue in years to come. As hydraulic fracturing occurs, accidental spills of highly saline produced water have severe impact on nearby soils. The release of large concentrations of salts into the soil profile can destroy plant and microbial life, as well as disperse soil clays causing erosion. Current remediation techniques for this problem, such as excavation or soil washing, are destructive or only partially effective. This study explores a novel technique using surface evaporation to draw salts in solution toward the soil surface when ferrocyanide is added to promote efflorescence. NaCl has the most potential to cause soil pore clogging due to its high concentration and ferrocyanide interacts with NaCl to form dendritic efflorescence that can be effectively removed. Beaker sand column experiments were conducted using produced waters from the Permian Basin to simulate spill sites. Prussian yellow was found to be the most effective form of ferrocyanide. The composition of the produced water was found to have large effect on the capability of Prussian yellow to induce efflorescence. Produced waters with higher background ion concentrations required ten times as much Prussian yellow to cause significant efflorescence. Alternatively, it was found that EDTA could be added to a produced water as a chelating agent to effectively reduce competition for the ferrocyanide ion so that it can promote NaCl efflorescence. Spectrophotometry was used to determine that on average 73% of the Prussian yellow added was removed from the sand profile with the efflorescence. PHREEQC was utilized to model speciation of ferrocyanide and EDTA

within the produced waters and this highlighted a need for a predictive model to determine the most efficient dosage of additives for a given produced water spill.

## Chapter 1

### INTRODUCTION

Hydraulic fracturing has revolutionized the onshore energy industry. While current practices are designed to prevent spills during operations, every year accidents occur that can contaminate local soils with highly saline produced water (PW). The salts from spills can affect soil fertility and disperse soil clays, which can result in plant death and increased erosion and water runoff. Commercially available technologies to remediate brine impacted soils are time consuming, costly, and only partially effective. In this research, a novel technology is evaluated that removes salts from contaminated soil through an enhanced evaporative flux.

Surface water evaporation and capillary action transport saline water upwards through the soil (Figure 1A and 1B). As water content decreases near the surface due to evaporation, salt concentrations effectively increase. This process is enhanced by the presence of a crystallization modifier which prevents salts from precipitating below ground (subflorescence in Figure 1C) and clogging soil pores as the water evaporates. This allows the salts to crystallize above the soil surface (efflorescence in Figure 1D) where they can be easily physically removed.

The primary component of most PWs is NaCl. Ferrocyanide,  $\text{Fe}(\text{CN})_6^{4-}$ , is a well-known crystallization modifier for NaCl. It has been utilized for many years to prevent infrastructure damage due to NaCl crystallization in building materials (Gupta et al., 2012; Lubelli and van Hees, 2007; Rodriguez-Navarro et al., 2002). The application of this methodology to brine-ridden soils was introduced in 2016 when it

was found that NaCl saturated soil columns produced 46-57% salt efflorescence with 1-10 mM ferrocyanide presence (Daigh and Klaustermeier, 2016).

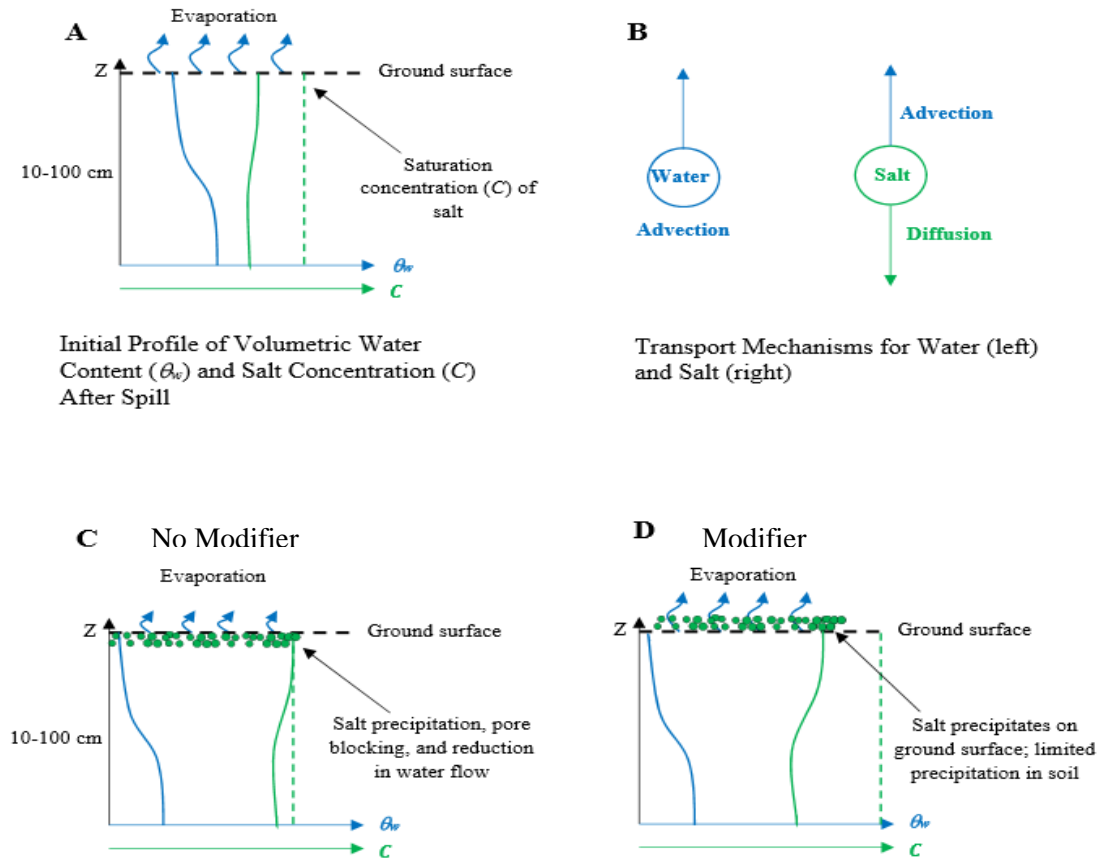


Figure 1: (A) Schematic of the soil profile at a brine-contaminated site showing water and salt concentration gradients. (B) Salts are expected to move upwards within the soil along with the advection of water. (C) Clogging of soil pores without inhibitor vs. (D) efflorescence on the soil surface with inhibitor.

The mechanisms of ferrocyanide's interaction with NaCl are still being explored. It acts as both a nucleation inhibitor and habit (crystal shape) modifier. It is

believed that the nucleation inhibition is due to ferrocyanide's affinity to solvate, thus decreasing water content for the salt to dissolve in, and ferrocyanide's ability to adsorb  $\text{Na}^+$  ions which interferes with NaCl formation (Rodriguez-Navarro et al., 2002). The growth modification is believed to be an effect of the  $\text{Fe}(\text{CN})_6^{4-}$  ion's ability to take the place of a  $\text{NaCl}_6^{5-}$  cluster in the crystal lattice due to their similar size and octahedral structure (Bode et al., 2012). The charge mismatch which is induced by this replacement prevents further step growth of the crystal. The kinetic roughening caused by this phenomenon lowers surface energy and increases supersaturation, effectively inhibiting growth and modifying crystal habit (Townsend et al., 2017). The typically cubic, face-centered NaCl crystal changes to a dendritic crystal as the ferrocyanide adheres to the {100} face of the NaCl, thus promoting growth of the other {110} and {111} faces (Rivas et al., 2010). While the cubic crystal can easily clog soil pores, the smaller dendritic crystal likely fills a smaller portion of pores allowing liquid movement through "creep" across the crystals' branches and large surface area (Gupta et al., 2014; Townsend et al., 2016). It is a combination of these physical and chemical processes that gives ferrocyanide its ability to promote surface salt efflorescence.

While much research has examined ferrocyanide's interactions with pure NaCl solutions, very little is known of its effects in mixed electrolyte solutions. This idea began to be explored with solutions that had both NaCl and either KCl or LiCl (Gupta et al., 2015), but PWs have such complicated chemistries that even these solutions are potentially not directly useful. To fully assess the efficacy of this technique to remediate fracking brine spills, it needs to be tested with real PWs. For this study, two PWs were collected from the Midland and Delaware regions of the Permian Basin and were chemically characterized for ion composition. Chemical speciation modeling was

paired with experimental batch and sand column evaporation tests to develop an understanding of the effects of the presence of background ions on the interaction between NaCl and ferrocyanide. PHREEQC was utilized as a state of the art chemical equilibrium modeling computer program to aid in solving the equilibrium speciation in the aqueous solutions (Parkhurst, D.L., Apello, 1999). If this technique continues to prove effective, the next step is the development of a chemical model and its incorporation into a more complete reactive mass transport model. This would be used to evaluate the applicability of this technology to various PW compositions and soil characteristics.

## Chapter 2

### MATERIALS & METHODS

#### 2.1 Produced Waters and Crystallization Modifiers

Samples of PW from the Delaware and Midland basins, sub-basins within the larger Permian basin, were supplied by ExxonMobil. The Delaware basin is located mostly in Texas and partly in New Mexico and the Midland is located solely in Texas. Samples from three different tank batteries within each basin were collected and mixed to obtain a representative water for each. The Delaware basin PW was collected from the James Ranch, Big Eddy, and Remuda/Poker Lake units. The Midland basin PW came from three Midkiff/Endeavor units (100, 200, and 400). At each of the facilities sampled, PW was collected from multiple nearby wells and thus represent a composite of the area. These waters were stored in 5-gallon polyethylene carboys at 5°C and filtered through a 0.45 µm mixed cellulose ester filter before use in experiments.

Subsamples of each mixture were sent to Alpha Analytic Labs (Westborough, MA) for chemical analysis, the results of which are found in Table A1 in Appendix A. Despite the proximity of the basins, their PWs were found to have significantly different compositions. Their compositions were compared to PWs in other states using data from the USGS National Produced Waters Geochemical Database v2.3 (Blondes et al., 2018). This database has over 114,000 lines of data that were filtered to include only the waters that were marked specifically as “produced” and that had the required elemental analysis for comparison (Na, Cl, Ca, Fe, K, Mg, Ba, pH).

Figure 2 displays the results of some of the more prevalent ions:  $\text{Ca}^{+2}$ ,  $\text{Cl}^-$ , and  $\text{Na}^+$ . Along with the two basins included in this study, basins from five other states were analyzed for average compositions. Produced water composition varies greatly with geographic region due to differing geologic formations so it will be important to understand the characteristics of the spill at hand.

The Delaware PW used in this study is on the high end of the concentration ranges for most ions. The Midland PW seems to have more average concentrations. Oklahoma, Texas, New Mexico, and Illinois have similarly high concentrations while Wyoming and Colorado are much less concentrated. The ions other than sodium and chloride, such as calcium, that could potentially cause competition within the PWs are also important. There are many other hydraulic fracturing states across the USA that will have other compositions, and the wide range of concentrations highlights the need for a model to accompany this remediation technique. Acknowledging these compositional differences when designing a remediation plan will allow for more precise applications of ferrocyanide or other crystallization modifiers. Comparisons for the other ions and pH can be found in Table A2.

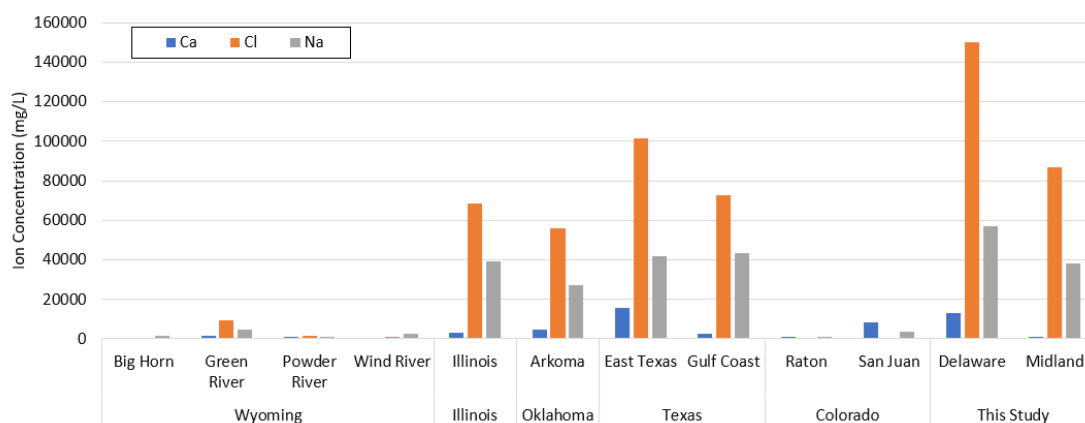


Figure 2: Comparison of  $\text{Ca}^{+2}$ ,  $\text{Cl}^-$ , and  $\text{Na}^+$  concentrations found in produced waters in various basins across the United States.

To alter the crystallization of these PWs as evaporation occurred, ferrocyanide was used as both a growth modifier and nucleation inhibitor. The three forms of ferrocyanide tested include Prussian yellow,  $\text{K}_4\text{Fe}(\text{CN})_6 \cdot 3\text{H}_2\text{O}$  (Alfa Aesar), Prussian blue,  $\text{Fe}_4(\text{Fe}(\text{CN})_6)_3$  (Acros Organics), and a combination of Prussian blue with 0.033 M ammonium hydroxide (Fisher Scientific). For the majority of experiments the Prussian yellow form was used.

## 2.2 Experiments Evaluating PHREEQC Model

To validate the chemical speciation modeling performed in PHREEQC and discussed in Section 2.6, lab evaporation experiments were conducted. Both PWs and two reagent grade NaCl solutions, 3.8 M and 2.16 M NaCl corresponding to NaCl concentrations in the Delaware and Midland basins, respectively, were placed in 425 mL beakers inside a 15 L recirculating water bath (Polyscience SD15R-30-A11B). These NaCl solutions were used to compare the results obtained from the PWs which have much more complicated water chemistries. The bath was set to 60°C to induce

rapid evaporation, and overhead stirrers mixed the 160 mL solutions (initial volume) at 220 rpm to ensure homogeneity. The beakers were weighed and solution electroconductivity was measured every 1-2 h. Electroconductivity measurements were taken using Mettler Toledo's InLab 738 ISM conductivity probe connected to the Seven2Go S3 portable conductivity meter. The conductivity measuring range for this meter is 0.010  $\mu\text{S}/\text{cm}$  – 500  $\text{mS}/\text{cm}$ , with a  $\pm 0.5\%$  accuracy, making it ideal for such concentrated brines. Two duplicates of each solution were included.

### **2.3 Sand Experiments**

Four sets of column experiments were performed to evaluate the precipitation of salts during evaporation of brine-contaminated media and the utility of crystallization modifiers for reducing soil clogging. Experiments were conducted in 250 mL low form Fisherbrand Griffin beakers. A well-characterized, uniform 30/40 Accusand (Schroth et al., 1996) from Covia Corporation was used as a model porous medium. This sand was further sieved to 30/35 size, washed, and oven-dried. The sand was wet-packed with 30 mL of the desired solution so that a partially saturated profile was created. The average porosity of the columns was  $42.5 \pm 0.5\text{SE}\%$  (SE = one standard error of the mean). To prevent pooling of solution on the surface, a dry layer of sand was also present at the very top of the sand profile. On average,  $67.3 \pm 1.4\text{SE}\%$  of the pore space was filled with solution at the start of each experiment. These conditions represent a recent spill, with the solution remaining close to the surface. The column of sand was  $3.21 \pm 0.03\text{SE}$  cm in height. The solutions used were the 3.8 M NaCl solution, the Delaware basin PW, and the Midland basin PW, with the PWs being filtered prior to use. Trials with ferrocyanide and with EDTA additions had the

chemicals added directly to the solution in the desired concentration and were mixed on a stir plate prior to packing the solution into the sand column. Columns were left to evaporate naturally in a 21-23°C controlled lab environment. The columns were left for approximately three weeks, with the mean duration being  $20.3 \pm 0.2SE$  days. Humidity varied with outdoor weather conditions and ranged from 55 – 70% relative humidity.

After evaporation, columns showing salt efflorescence were surface-scraped to remove salt that had effectively been removed from the sand column. A stainless steel scoopula was used to carefully separate loose salt crystals from the top sand layer, without disrupting salts still beneath the surface. Any salts that had formed a hard crust and could not be easily separated were considered subflorescence and were not removed. The salts were dissolved in 100 mL DI water and the remaining sand column was stirred in 500 mL DI water. Electroconductivity measurements of the surface and sand solutions were taken to determine the ratio of salt removed to that remaining in the column. The measurements were compared to a calibration curve for each solution made to convert electroconductivity to salt molarity (Figure A1).

The first sand column trial tested the efficiency of three different NaCl crystal modifiers on the three brines: 3.8 M NaCl, Delaware PW, and Midland PW. The three modifiers were Prussian yellow, Prussian blue, and a combination of Prussian blue with 0.033 M ammonium hydroxide. The ammonium hydroxide addition is known to partially or fully ionize the  $Fe^{+3}$  from the ferrocyanide ion because Prussian blue is a much more insoluble form of ferrocyanide compared to Prussian yellow (Daigh and Klaustermeier, 2016). The modifiers were added to the solutions in 0, 1, and 10 mM concentrations.

After determining that Prussian yellow was the superior form of the ferrocyanide, a second set of experiments tested the effects of small changes in Prussian yellow concentration. The modifier was applied in 0, 1, 1.5, 2, 3, 5, 7, and 10 mM concentrations to the Delaware and Midland PWs and then packed into sand columns for evaporation.

The third trial focused on the 1 mM concentration of Prussian yellow and tested the effects of adding Ethylenediaminetetraacetic acid (EDTA) in the form  $\text{Na}_2\text{EDTA}\cdot 2\text{H}_2\text{O}$  (Acros Organics) to the brines. EDTA was added in 0, 10, 50, 100, and 200 mM concentrations to the Delaware and Midland PWs. These solutions were then sand-packed for evaporation. The EDTA is expected to complex the background ions competing with the NaCl for free ferrocyanide ( $\text{Fe}(\text{CN})_6^{4-}$ ) ions.

The last trial also tested 1 mM Prussian yellow concentrations with additions of EDTA in each of the PWs. EDTA was applied in 0, 1, 5, 10, 50, and 100 mM concentrations. However, this time when the EDTA was added, the pH was readjusted back up to a neutral pH of approximately 7. The pH readjustment was performed through additions of sodium hydroxide. A table of solution pHs can be found in Appendix A (Table A3).

#### **2.4 Spectrophotometric Analysis of Ferrocyanide Fate**

To gain an understanding of the fate of the ferrocyanide within the sand columns, Prussian yellow's light absorbing properties were utilized and spectrophotometry was applied. The solutions that were created from diluting the surface scraped salts in 100 mL DI water and the remaining sand column in 500 mL DI water were subsampled after electroconductivity readings were taken. These

subsamples were diluted further as required and absorbance was measured using a Shimadzu UV-1280 spectrophotometer at a wavelength of 220 nm. This wavelength was found to be the peak absorption for Prussian yellow samples dissolved in DI water as reported in the literature (Glasner and Zidon, 1974). A calibration curve was created using known concentrations of Prussian yellow in DI water to convert absorbance to Prussian yellow molarity (Figure A2). Background absorbances due to differing matrices of NaCl and PW rather than DI water were found to be minimal so that no matrix corrections were made. Sand columns containing EDTA were not included in this analysis as EDTA was found to have more significant effects on absorbance readings and Prussian yellow recovery rates were too inaccurate to report.

## **2.5 Solution Evaporation Experiments**

To evaluate the effects of Prussian yellow on crystal morphology, sand-free beakers were also assembled. Smaller 100 mL glass beakers were filled with 30 mL of a given brine (3.8M NaCl, Delaware PW, or Midland PW), both with and without additions of Prussian yellow. The same 0, 1, and 10 mM modifier concentrations were used. Photos (Apple iPhone XR) and scanning electron micrography (SEM) images (JEOL JSM-7400F SEM) were taken of the crystals formed after complete evaporation. These images allow comparison of particle shape and size with and without chemical modifier present during crystallization.

## **2.6 PHREEQC Modeling**

The geochemical equilibrium speciation software, PHREEQC was used to model chemical reactions within the PWs during evaporation. The Pitzer database was utilized that can reliably compute chemical activity in solutions with high ionic

strength (Plummer and Parkhurst, 1990). The PW ion concentrations were the input solution parameters. A reaction block was included to remove moles of water from the initial solution to simulate evaporation. Solution characteristics, such as salt saturation indices, precipitation volumes, and electrical conductivities were monitored as evaporation progressed. This allowed for determination of which salts would precipitate and potentially cause soil clogging.

The software was also used to help understand the speciation of ferrocyanide and EDTA upon addition to the PWs. The Pitzer database does not have the capability to compute the activity corrections for ions with -4 charges, required for the ferrocyanide ( $\text{Fe}(\text{CN})_6^{-4}$ ) anion. For this reason, the Minteq database (Allison et al., 1991) was utilized that employs the Davies activity equations (Davies, 1962). These equations are reliable up to 0.5 to 2 M concentration range in PHREEQC. To conform to this limitation, the composition of the PWs used in the modeling was changed by decreasing the concentrations of sodium and chloride, the two ions present in highest abundance, to 0.1 M. All other ions were kept at their actual concentrations and 1 mM ferrocyanide was added to simulate a beaker trial. Using a reaction block, up to 240 mM EDTA was titrated into the solution and the competition among ions for the free EDTA and free ferrocyanide ions was predicted.

## Chapter 3

### RESULTS

#### 3.1 Evaluation of PHREEQC Model

Using PHREEQC to model the PWs during evaporation, the saturation indices (*SI*s) of each salt were predicted. For NaCl, *SI* is computed from (Thiel et al., 2015)

$$SI = \log \frac{\{Na^+\}\{Cl^-\}}{K_{sp}} = \log \frac{\gamma_{Na^+}[Na^+]\gamma_{Cl^-}[Cl^-]}{K_{sp}} \quad (1)$$

where  $\{Na^+\}$  and  $\{Cl^-\}$  refer to the element's activities which are equal to the element's concentrations,  $[Na^+]$  and  $[Cl^-]$ , multiplied by their respective activity coefficients  $\gamma_{Na^+}$  and  $\gamma_{Cl^-}$ . When the *SI* increases to a value of zero or above, salt is expected to precipitate. This is due to the activity product of the ions becoming equal to or greater than the salt's solubility product,  $K_{sp}$ .

PHREEQC model predictions for the two different basins produce quite different results. Figure 3A (Delaware) and 3B (Midland) show that both PWs are initially expected to precipitate barite ( $BaSO_4$ ), celestite ( $SrSO_4$ ), and ferrihydrite ( $FeOH_3$ ), exemplified by their  $SI = 0$ . The Delaware is expected to begin precipitating  $MgCl_2 \cdot 2H_2O$  at 7% evaporation while the Midland does not begin until 62%, due to lower Mg and Cl concentrations. Both PWs show that barite and celestite eventually stop precipitating, due to changing concentrations as halite (NaCl) reaches its saturation point. The start of halite precipitation occurs at approximately 44% evaporation for the Delaware and much later at approximately 67% evaporation for the Midland. This difference is caused by the PWs' varying compositions with the

Midland having only about two thirds the chlorine and sodium concentrations of the Delaware (see Table A1). Based on Figure 3A and 3B, barite and celestite might be expected to be the salts of concern because they precipitate first and would thus begin clogging soil pores earlier. However, when the volume of the precipitated salts (Figure 3C and 3D) are considered, halite is produced in much larger quantities than all the other salts combined and thus has the most ability to clog soil pores. Using 80% evaporation as a comparison point, halite constitutes more than 90% of the salts precipitated for both basins. However, to highlight how much more concentrated the Delaware PW is, at 80% evaporation, the Delaware is expected to precipitate 63 cm<sup>3</sup> of halite per liter of brine, while the Midland prediction is only 23 cm<sup>3</sup>/L.

The halite concentration in solution accounts for essentially all of the measured electroconductivity and thus measured changes in conductivity can be used as a proxy for absence or presence of halite. Figure 3E and 3F show both experimental and model results of electroconductivity trends in the evaporating brine solutions. In all of the solutions, the electroconductivity steadily increases as evaporation occurs until reaching a plateau and then flattening out as precipitation continues. Experimentally, the plateau is seen at 44% evaporation for the Delaware PW and 72% evaporation for the Midland PW. The point of plateau for the Delaware matches exactly with the PHREEQC plateau predictions and they align with the point in evaporation where halite is expected to reach  $SI = 0$  and begin precipitating, as indicated by the dashed purple vertical line. The Midland PW's plateau does not match PHREEQC quite as accurately. The experimental plateau occurred at 72% evaporation while the model plateau and halite  $SI = 0$  was predicted at 67%. This is only a 5% offset which is a

reasonable error and could be due to slight inaccuracies in PW composition and the approximate relationship can be seen by the purple vertical line.

There is a slight offset between the model and experimental conductivity readings, with the model always predicting higher conductivities. The offset worsens as more evaporation occurs which suggests it is likely due to inaccuracies of the model as the ionic strength reaches extremely high values due to decreased water content, effectively surpassing the limitations of the software's predictive capabilities.

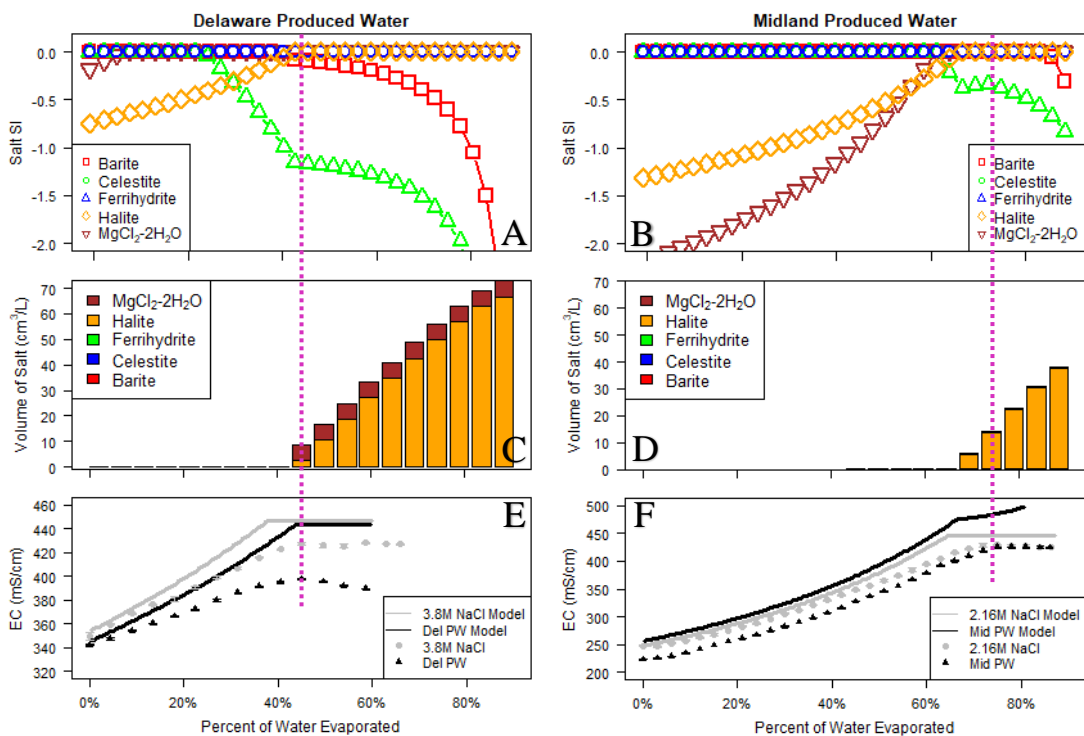


Figure 3: PHREEQC modeling of changes in the salt saturation indices and precipitate salt volumes ( $\text{cm}^3$  of salt per liter of brine) with increasing evaporation. A) Delaware SI, B) Midland SI, C) Delaware volumes, D) Midland volumes. Followed by the experimental results of electroconductivity changes during evaporation in the E) Delaware and F) Midland.

These results indicate that electroconductivity has good potential for use as a proxy for NaCl presence and precipitation. For example, a conductivity probe could be installed at a spill site to predict when NaCl precipitation will begin based on changes in conductivity readings. The calibration curve created for the relationship between changes in NaCl molarity and conductivity can be found in Figure A1.

## **3.2 Sand Experiments**

### **3.2.1 Comparing Ferrocyanide Forms**

To visualize the results of the sand column trials with varying forms of ferrocyanide, photos of the salts after evaporation are shown in Figure 4. Without any ferrocyanide addition (0 mM), the salts are unable to effloresce on the surface. With Prussian yellow present at 1 mM, the 3.8 M NaCl and Midland PW effloresced while in contrast, the Delaware PW did not. The 3.8 M NaCl has a similar amount of NaCl as the Delaware PW, so any difference in outcome is due to the presence of competing ions in the PW. At 10 mM Prussian yellow, all three brines show fluffy, dendritic efflorescence, suggesting that the extra Prussian yellow was able to overcome the competition of the other ions in the Delaware PW.

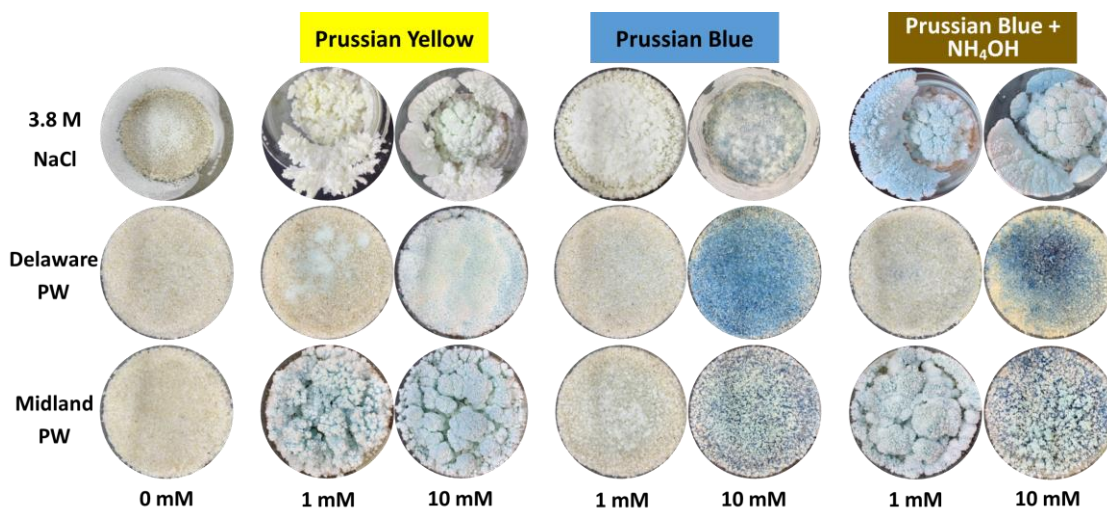


Figure 4: Top view of sand column beakers without any modifier (0 mM) and with varying forms of ferrocyanide (Prussian yellow, Prussian Blue, and Prussian Blue +  $\text{NH}_4\text{OH}$ ) at 1 and 10 mM concentrations. Images taken after 21 days of evaporation.

Prussian blue alone was unable to produce removable efflorescence in any of the columns, as shown in Figure 4. There were minimal salts on the surface at the 1 mM and 10 mM Prussian blue concentration for 3.8 M NaCl and at the 10 mM concentration for the Midland PW, but these salts formed a hard crust and were unable to be separated from the sand. These beakers are indicated with a blue asterisk in Figure 5. This confirms that to dissociate Prussian blue into the  $\text{Fe}^{+3}$  and the free ferrocyanide ion, another compound, such as  $\text{NH}_4\text{OH}$  must be present. On the other hand, the  $\text{K}^+$  ions in Prussian yellow easily dissociate when dissolved in solution, allowing the free ferrocyanide to interact with the NaCl and produce efflorescence. The Prussian blue plus  $\text{NH}_4\text{OH}$  combination was effective in producing efflorescence, within 2% of the efficiency of Prussian yellow in all, but two beakers: the 10 mM Delaware and Midland (Figure 5). The 10 mM Delaware had 86% efflorescence with

Prussian yellow, but 0% efflorescence with Prussian blue plus  $\text{NH}_4\text{OH}$ . The 10 mM Midland had 89% efflorescence with Prussian yellow, but only 24% efflorescence with Prussian blue plus  $\text{NH}_4\text{OH}$ . The inferiority of Prussian blue is hypothesized to be due to the inability of Prussian blue to dissociate in such complex solutions. A brown precipitate also formed upon addition of  $\text{NH}_4\text{OH}$ , which is believed to be an iron hydroxide. The iron precipitate could potentially add to pore clogging issues. These results suggest that the Prussian blue form of ferrocyanide is less desirable to work with. Some of the sand columns were also dyed blue after the evaporation, which would be undesirable in the environment.

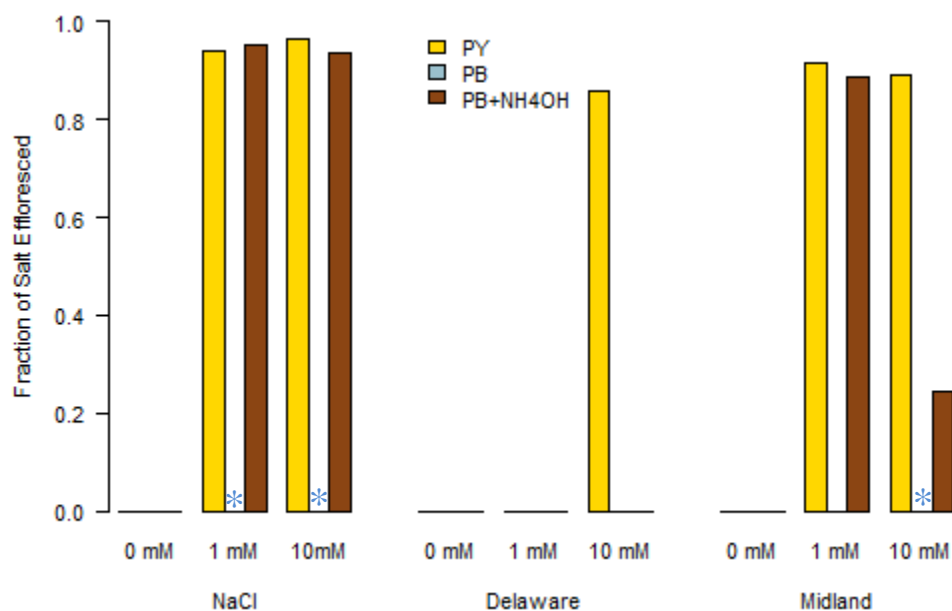


Figure 5: The effects of Prussian yellow (PY), Prussian Blue (PB), and Prussian Blue + 0.033 M  $\text{NH}_4\text{OH}$  on salt column efflorescence. All three brines, 3.8 M NaCl, Delaware PW, and Midland PW were tested at 0, 1, and 10 mM ferrocyanide concentrations. An \* signifies a beaker that produced crystallization on the surface, but formed a hard crust that was impossible to separate from the sand column.

Prussian yellow was found to be the most effective form of ferrocyanide. When a column does effloresce in the presence of Prussian yellow, over 80% of the salts are effectively removed from the sand, making this a very efficient process.

### 3.2.2 Prussian Yellow Sand Columns

All follow-on experiments were performed with the Prussian yellow form of ferrocyanide. Figure 6 provides a side view and top view of columns with Prussian yellow and either 3.8 M NaCl, Delaware PW, or Midland PW. The shape and height of the crystals can be more easily visualized in this presentation. It appears that the more complicated chemistry in the PWs prevents their salts from creeping quite as high, compared to the pure NaCl salts.

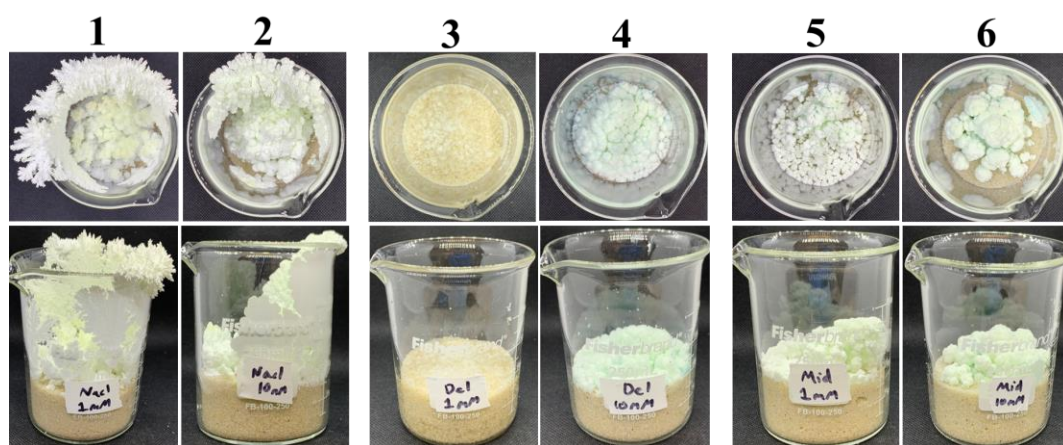


Figure 6: Sand column photos for the beakers with 1mM and 10 mM Prussian yellow additions. Top row gives top view of beakers while bottom provide profile views. Columns 1+2) 3.8 M NaCl, 3+4) Delaware PW, 5+6) Midland PW

Beakers were then set up with 0, 1, 1.5, 2, 3, 5, 7, and 10 mM Prussian yellow concentrations (Figure 7). Over the range of ferrocyanide concentrations tested, the Midland shows stable efficiency, always obtaining 76-92% efflorescence. Even with the minimum 1 mM concentration added, the Midland showed an average of 90.8 +/- 0.3SE % efficiency. This average and standard error were determined from 5 replicate beakers from 4 different trials, exemplifying the good reproducibility of this procedure. The Delaware does not begin showing any efflorescence until 2 mM Prussian yellow is added, requiring double the ferrocyanide addition compared to the Midland. At 2 mM Prussian yellow, only 65% of the salt effloresces. This percentage slowly increases as more ferrocyanide is added, reaching 69% removal at 7 mM Prussian yellow, still below the efficiency of the Midland. With a 10 mM Prussian yellow addition, the Delaware shows an abrupt increase to 88% efflorescence, effectively requiring ten times as much Prussian yellow to match the removal percentage of the Midland. The data shows good reproducibility, with duplicate trials having a difference of about 3% or less. The only exception is a single case, a 2 mM Midland beaker which produced 61% efflorescence, much lower than any of the other concentrations. This outlier was removed from the graph as an anomaly. The Prussian yellow clearly shows a marked difference in efficiency for the Delaware versus the Midland PW and again indicates a need for a model.

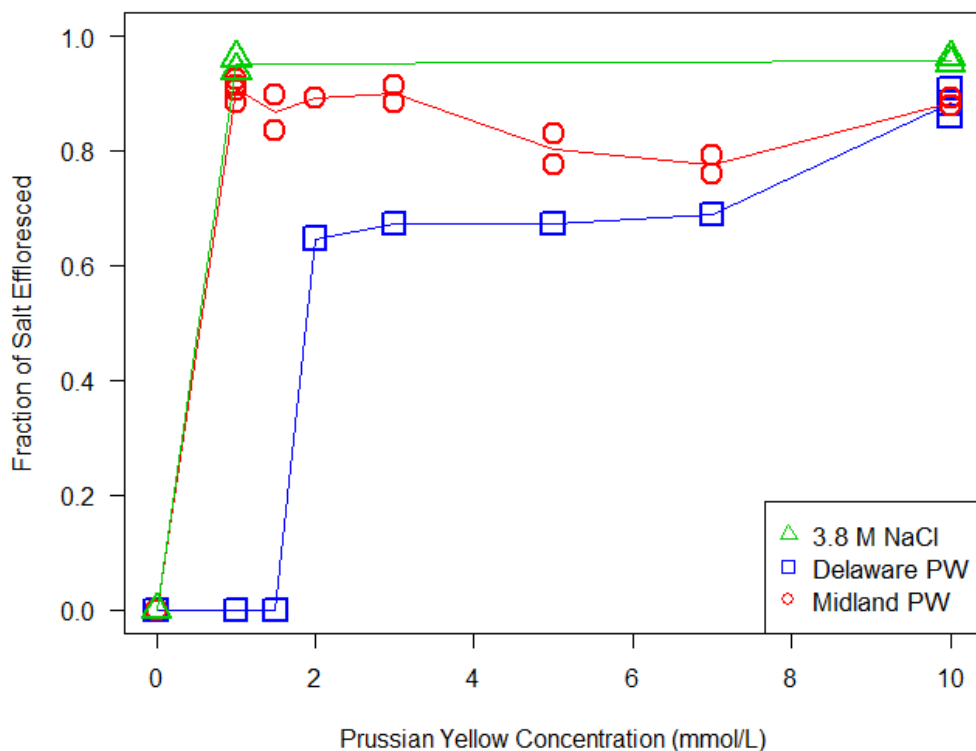


Figure 7: Surface salt efflorescence of sand columns with varying concentrations of Prussian yellow for NaCl, Delaware PW and Midland PW.

### 3.3 Spectrophotometric Analysis of Ferrocyanide Fate

While this process already has its merits as a non-destructive in situ remediation technique, it would be more desirable if the Prussian yellow added to the sand was effectively removed with the salts. To investigate the fate of the ferrocyanide, spectrophotometry was used at a 220 nm wavelength. Data are shown for 18 beakers and range from 58.1% to 88.8% ferrocyanide removal, with the average being  $73.2 \pm 0.6SE$  % (Figure 8). This suggests that a majority of the modifier added is removed again along with the undesired salts. There does not seem to be a major trend between fraction of salt effloresced and fraction of Prussian yellow in the salt.

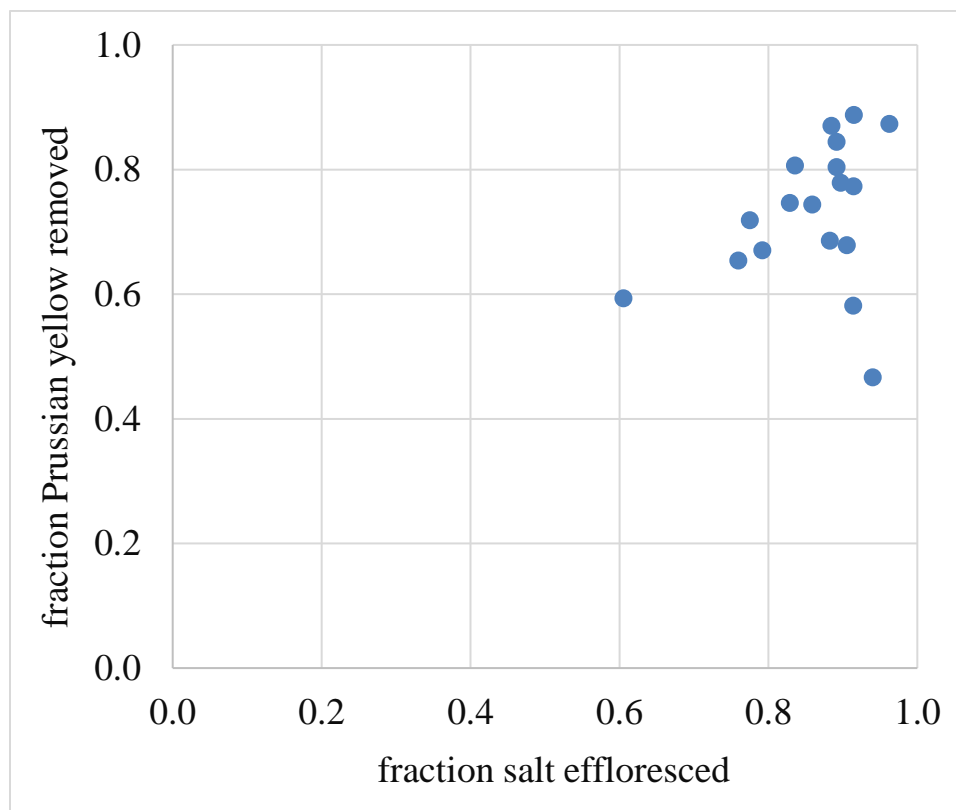


Figure 8: Spectrophotometry results for fraction of Prussian yellow removed with effloresced salts versus fraction of salt effloresced.

Although not pictured, there does not seem to be a relationship between fraction of Prussian yellow removed and amount of Prussian yellow added. The spectrophotometry seems to be effective in capturing all of the Prussian yellow present in the beakers. When comparing added versus recovered moles of Prussian yellow (Figure A3) the mean square error was only 0.43  $\mu\text{mol}$  when a range of 0 - 300  $\mu\text{mol}$  were added.

### 3.4 Solution Evaporation Experiments

To gain a better view of the processes occurring below the sand surface, salts were grown in beakers without sand. This was a simple procedure where 30 mL of each solution was left in a beaker for a few weeks until complete evaporation occurred. Figure 9 shows the differing shapes of salts formed with and without Prussian yellow. Without ferrocyanide addition, the sodium chloride forms into the typical cubic, face-centered crystals with clearly defined, sharp edges (Townsend et al., 2017). These large crystals can be seen with the human eye and have a typical length of up to 0.4 cm in size. These particles could easily clog sand pores (diameter of sand = 0.532 mm) and prevent the removal of the salts from the sand column. With the addition of 1 mM Prussian yellow, the 3.8 M NaCl and Midland both show a similar change in morphology, producing fluffy, dendritic crystals, with many having a diameter less than 10  $\mu\text{m}$ . The Delaware also shows a difference in morphology with Prussian yellow presence, although quite different from the other two brines. The crystals no longer have a defined cubic shape, but they are not fluffy dendrites either. The crystals formed a flat layer in the bottom of the beaker and still show great capability to clog soil pores, with some crystals still having a diameter of at least 400  $\mu\text{m}$ . When 10 mM Prussian yellow is added however, all three brines show a fluffy dendritic morphology. The SEM images show that there are still small differences in morphology with the pure sodium chloride having sharper edges and the PWs having more rounded edges, likely due to other impurities present from the complicated PW composition. These images provide further confirmation that the free ferrocyanide ion is being complexed by other ions in the Delaware PW, preventing it from interacting with the NaCl.

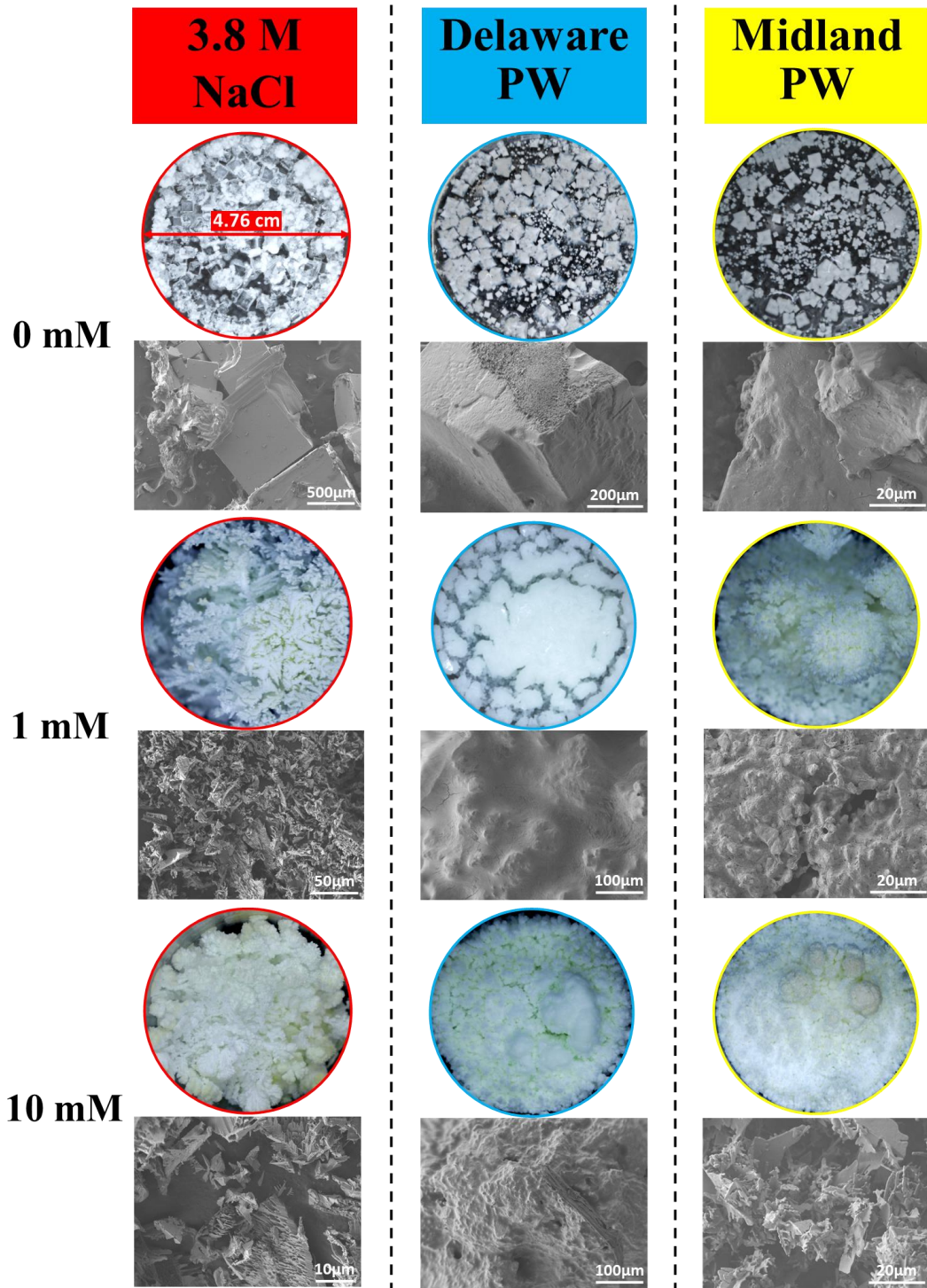


Figure 9: Camera (circles) and SEM (rectangles) images of salts formed in beakers of 30mL of 3.8M NaCl, Delaware, or Midland produced waters. Showing effects of adding 0, 1, or 10 mM Prussian yellow.

### 3.5 EDTA Sand Column Experiments

To effectively remove some of the competing ions from the PW, EDTA was added as a chelating agent. EDTA can form four or six bonds with cations, making it extremely efficient. The pKa's for the  $\text{Fe}^{+3}$ -EDTA,  $\text{Ca}^{+2}$ -EDTA, and  $\text{Na}^{+}$ -EDTA complexes are 25.1, 10.69, and 1.66, respectively. This makes it an ideal chelator to bind competing ions while leaving sodium ions free to bind with the ferrocyanide. Initially at the 1 mM Prussian yellow concentration, the Delaware does not produce any efflorescence. With the additions of EDTA as a chelating agent however, efflorescence is seen at this concentration (Figure 10).

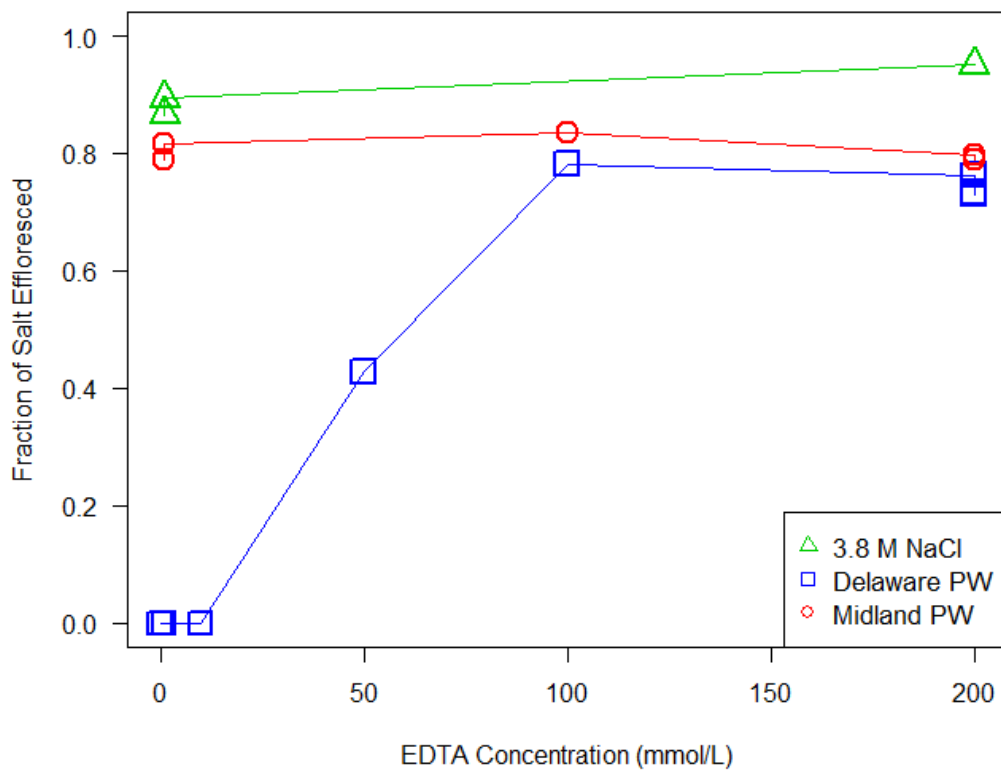


Figure 10: Surface salt efflorescence of sand columns with varying concentrations of EDTA. Data shown for columns with 3.8 M NaCl, Delaware PW, and Midland PW. All columns had 1 mM Prussian yellow.

At 50 mM EDTA, salt begins to minimally effloresce on the surface, but only about 43% salt removal is achieved. Increasing EDTA to 100 mM, 78% removal is achieved, slightly greater than the 69% removed with the addition of 7 mM Prussian yellow alone.

These results suggest that there are cations in the PW that are forming cation-ferrocyanide ion complexes that lower the concentration of the free ferrocyanide ion and reduce its interaction with the NaCl crystals. When the competing ions are complexed by the EDTA, the ferrocyanide is free to induce surface efflorescence of the NaCl crystal. The possible mechanisms are either  $\text{Fe}^{+3}$  is present in the PW, creating a form of Prussian blue, or the high concentration of  $\text{Ca}^{+2}$  forms a Ca-ferrocyanide complex, or a combination of both.

A small set of sand column experiments were performed with the pH readjusted to neutral after addition of EDTA to the PW. The 1 mM Prussian yellow concentration was still used for all beakers. These experiments produced surprising results in comparison to EDTA experiments without pH adjustment. The Delaware PW reacted similarly showing minimal efflorescence until 100 mM EDTA additions, where it achieved approximately 80% salt removal. The Midland PW however, showed decreasing efflorescence as more EDTA was added. These results are shown in Figure 11.

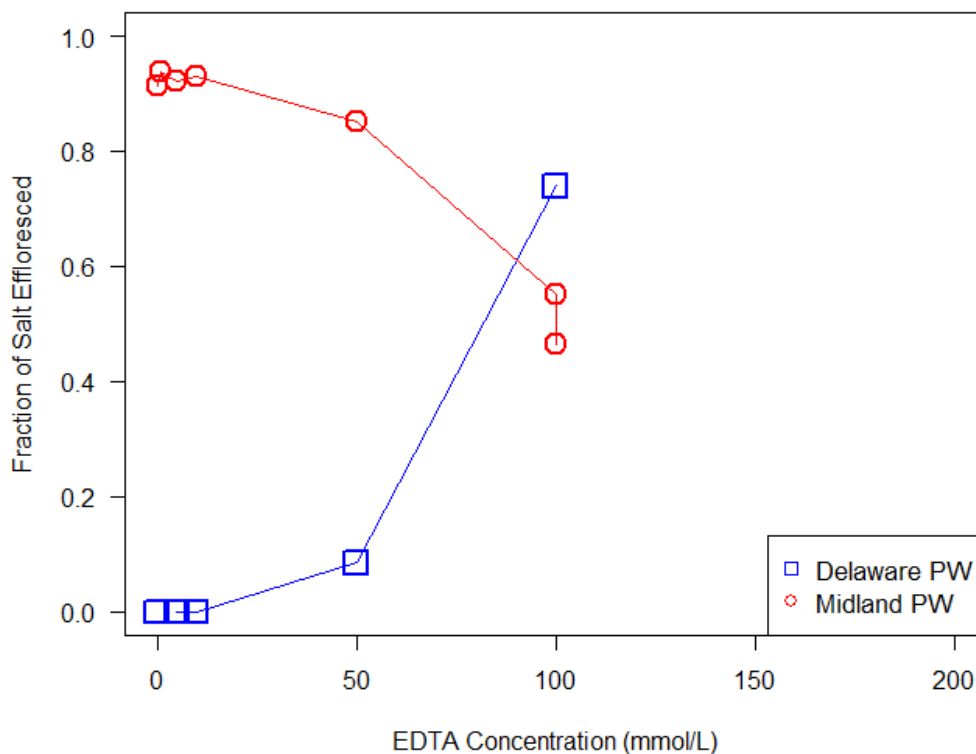


Figure 11: Surface salt efflorescence of beakers with varying amount of EDTA that were pH adjusted to neutral pH. Data shown for the Delaware and Midland PWs. All with 1 mM Prussian yellow.

Exploring the mechanism that causes this phenomenon was out of the scope of this study. However, the results were included to highlight that solution and soil pH may be a factor to consider in the efficiency of this technique.

### 3.6 PHREEQC Modeling

The addition of EDTA to the PWs was modeled in PHREEQC with 1 mM ferrocyanide presence. The only alteration to the PW compositions was the NaCl concentrations were diluted to 0.1 M to stay within the limits of the activity corrections made with the Minteq database. Figure 12 shows that with no EDTA

additions, the majority of the 1 mM ferrocyanide is complexed with calcium and only 0.031 mM is complexed with sodium. On the other hand, the Midland PW has 0.38 mM of Na complexed ferrocyanide, more than tenfold greater. Good efflorescence was seen in the Delaware sand columns only once 100 mM of EDTA was added. This matches reasonably well with the model which shows that at 100 mM EDTA, the Na complexed ferrocyanide has increased to a concentration of approximately 0.32 mM, close to the original Midland concentration. This relationship between the Delaware and Midland is depicted with the purple dotted lines connecting the two basins' Na-ferrocyanide complex concentrations. These results are understandable because the calcium concentration in the Delaware PW (0.327 M) is more than ten times that of the Midland PW (0.028 M). With such a high concentration of competing ion, the Delaware PW required the assistance of the EDTA to remove the competition.

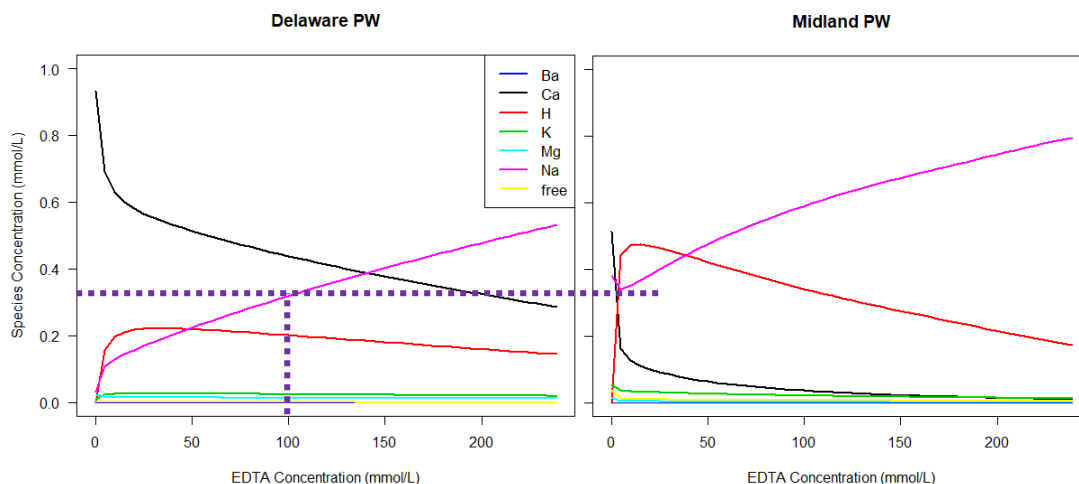


Figure 12: PHREEQC modeling of the speciation of 1mM ferrocyanide in the Delaware PW (left) and Midland PW (right). The speciation of the ferrocyanide ion is tracked as it creates complexes with Ba, Ca, H, K, Mg, and Na as EDTA is titrated into the solution as a chelating agent.

PHREEQC has provided clear insights into causes of the difference between the two basins' reactions to the 1 mM Prussian yellow concentration. To have a more complete model of the system, sorption of ferrocyanide onto NaCl crystals would need to be considered. Instead, the Na-ferrocyanide solution complexes are used as a proxy for all associations between the two species. The iron-ferrocyanide complex was also excluded due to its absence from the Minteq database. However, hints of blue color in effloresced salts suggest that Prussian blue could be forming and removing some of the free ferrocyanide. The iron concentrations are only 0.31 mM and 0.02 mM in the Delaware and Midland PWs, respectively. These are about 1000 times lower than their calcium concentrations, so iron is expected to have minimal effects in comparison.

## Chapter 4

### DISCUSSIONS & CONCLUSIONS

The chemical composition of a PW has profound effect on ferrocyanide's ability to produce salt efflorescence. While the simple NaCl solution and Midland PW did effloresce at lower Prussian yellow concentrations, the more concentrated Delaware PW required higher concentrations or EDTA additions. Due to this, experiments using simple NaCl solutions are inadequate at predicting ferrocyanide's ability to remediate brine-contaminated media.

In future work it will be important to explore differing conditions in the experiments, such as soil type and depth/age of the spill. For this study, the Prussian yellow would have to be pre-added to all PWs in case of a spill occurrence or applied immediately, before any significant drying can occur. A recently reported experiment had a similar setup in 250 mL beakers, but only managed 50% NaCl efflorescence with 10 mM Prussian yellow in pure NaCl solutions, while we achieved 90% (Swallow and O'Sullivan, 2019). However, the ferrocyanide in Swallow's study was added to a pre-dried soil where salts had already crystallized, and the soil was only 30% sand. Similar to this, Klaustermeier et al. (2017) were only able to achieve 35% NaCl recovery at 1mM and 47% NaCl recovery at 10 mM. However, that study used Prussian blue plus ammonium hydroxide rather than Prussian yellow and used a sandy loam soil. It has been suggested that the more clay content and less sand content a soil has, the less effective the ferrocyanide is due to smaller soil pores and potentially more sorption (Klaustermeier et al., 2017; Swallow and O'Sullivan, 2019). A soil's cation

exchange capacity has the potential to add more ions to the brine which could bind the free ferrocyanide. Testing varying soil types with PW will be a critical next step.

In spills of PWs with high background ion concentrations, a framework will be needed to determine whether to increase Prussian yellow concentrations or add EDTA to the soil. Ferrocyanide has been determined to be a stable compound, but there is some concern about free cyanide ions being released into the environment through degradation. Although it was found that on average 73% of Prussian yellow was effectively removed with efflorescence, one way to combat the amount of ferrocyanide added would be to include EDTA additions in waters that have high background ion concentrations. EDTA is already present in common products such as toothpaste and shampoo. PHREEQC has proven itself an effective tool in predicting the required amounts of ferrocyanide or EDTA to induce efflorescence.

While Prussian yellow was shown to be effective in causing surface efflorescence in simpler solutions, EDTA has proven itself an effective addition to complex competing ions in more complicated solutions. Ultimately, with these two tools available, greater than 80% of salts were removed from all solution types. This highlights the promise of this approach as an effective, lower cost and non-invasive remediation technique.

## REFERENCES

- Allison JD, Brown DS, Novo-Gradac KJ. MINTEQA2/PRODEFA2, A Geochemical Assessment Model For Environmental Systems: Version 3.0 User's Manual. 1991.
- Blondes, M.S., Gans, K.D., Engle, M.A., Kharaka, Y.K., Reidy, M.E., Saraswathula, V., Thordsen, J.J., Rowan, E.L., Morrissey EA. U.S. Geological Survey National Produced Waters Geochemical Database v2.3. US Geol Surv Data Release 2018. <https://doi.org/10.5066/F7J964W8>.
- Bode AAC, Vonk V, Van Den Bruele FJ, Kok DJ, Kerkenaar AM, Mantilla MF, et al. Anticaking activity of ferrocyanide on sodium chloride explained by charge mismatch. *Cryst Growth Des* 2012;12:1919–24. <https://doi.org/10.1021/cg201661y>.
- Daigh ALM, Klaustermeier AW. Approaching Brine Spill Remediation from the Surface: A New In Situ Method. *Agric Environ Lett* 2016;1:1–4. <https://doi.org/10.2134/ael2015.12.0013>.
- Davies CW. Ion Association. London: Butterworths; 1962.
- Glasner A, Zidon M. The crystallization of NaCl in the presence of [Fe(CN)<sub>6</sub>]<sup>4-</sup> ions. *J Cryst Growth* 1974;21:294–304. [https://doi.org/10.1016/0022-0248\(74\)90018-9](https://doi.org/10.1016/0022-0248(74)90018-9).
- Gupta S, Pel L, Kopinga K. Crystallization behavior of NaCl droplet during repeated crystallization and dissolution cycles: An NMR study. *J Cryst Growth* 2014;391:64–71. <https://doi.org/10.1016/j.jcrysgr.2014.01.016>.
- Gupta S, Pel L, Steiger M, Kopinga K. The effect of ferrocyanide ions on sodium chloride crystallization in salt mixtures. *J Cryst Growth* 2015;410:7–13. <https://doi.org/10.1016/j.jcrysgr.2014.10.018>.
- Gupta S, Terheiden K, Pel L, Sawdy A. Influence of ferrocyanide inhibitors on the transport and crystallization processes of sodium chloride in porous building materials. *Cryst Growth Des* 2012;12:3888–98. <https://doi.org/10.1021/cg3002288>.
- Klaustermeier AW, Daigh ALM, Limb RF, Sedivec K. Crystallization inhibitors and their remediation potential on brine-contaminated soils. *Vadose Zo J* 2017a;16. <https://doi.org/10.2136/vzj2016.10.0095>.

- Klaustermeier AW, Daigh ALM, Limb RF, Sedivec K. Crystallization Inhibitors and Their Remediation Potential on Brine-Contaminated Soils. *Vadose Zo J* 2017b;16:vzj2016.10.0095. <https://doi.org/10.2136/vzj2016.10.0095>.
- Lubelli B, van Hees RPJ. Effectiveness of crystallization inhibitors in preventing salt damage in building materials. *J Cult Herit* 2007;8:223–34. <https://doi.org/10.1016/j.culher.2007.06.001>.
- Parkhurst, D.L., Apello T. User's guide to PHREEQC version 3 - a computer program for speciation, batch-reaction, one-dimensional transport, and inverse geochemical calculations. 1999.
- Plummer LN, Parkhurst DL. Application of the Pitzer Equations to the PHREEQE Geochemical Model, 1990, p. 128–37. <https://doi.org/10.1021/bk-1990-0416.ch010>.
- Rivas T, Alvarez E, Mosquera MJ, Alejano L, Taboada J. Crystallization modifiers applied in granite desalination: The role of the stone pore structure. *Constr Build Mater* 2010;24:766–76. <https://doi.org/10.1016/j.conbuildmat.2009.10.031>.
- Rodriguez-Navarro C, Linares-Fernandez L, Doehne E, Sebastian E. Effects of ferrocyanide ions on NaCl crystallization in porous stone. *J Cryst Growth* 2002;243:503–16. [https://doi.org/10.1016/S0022-0248\(02\)01499-9](https://doi.org/10.1016/S0022-0248(02)01499-9).
- Schroth MH, Istok JD, Ahearn SJ, Selker JS. Characterization of Miller-Similar Silica Sands for Laboratory Hydrologic Studies. *Soil Sci Soc Am J* 1996;60:1331–9. <https://doi.org/10.2136/sssaj1996.03615995006000050007x>.
- Swallow MJB, O'Sullivan G. Biomimicry of vascular plants as a means of saline soil remediation. *Sci Total Environ* 2019;655:84–91. <https://doi.org/10.1016/j.scitotenv.2018.11.245>.
- Thiel GP, Zubair SM, Lienhard V JH. An Analysis of Likely Scalants in the Treatment of Produced Water From Nova Scotia. *Heat Transf Eng* 2015;36:652–62. <https://doi.org/10.1080/01457632.2015.954923>.
- Townsend ER, Van Enkevort WJP, Meijer JAM, Vlieg E. Additive Enhanced Creeping of Sodium Chloride Crystals 2017;19:3107–15. <https://doi.org/10.1021/acs.cgd.7b00023>.
- Townsend ER, Swennenhuis F, Van Enkevort WJP, Meijer JAM, Vlieg E. Creeping: An efficient way to determine the anticaking ability of additives for sodium chloride. *CrystEngComm* 2016;18:6176–83. <https://doi.org/10.1039/c6ce01376g>.

## Appendix A

### SUPPORTING INFORMATION

Table A1: Produced Water Compositions (mg/L)

ANALYTE	DELAWARE	MIDLAND
<b>GENERAL PARAMETERS</b>		
pH	6.0	6.7
TOTAL SUSPENDED SOLIDS	100	290
NITROGEN, TOTAL KJELDAHL	618	713
NITROGEN, AMMONIA	570	686
TOTAL ORGANIC NITROGEN	48.0	27.0
PHOSPHORUS, TOTAL	0.605	0.110
<b>MAJOR CATIONS</b>		
SODIUM, TOTAL	57200	38000
CALCIUM, TOTAL	13100	1120
MAGNESIUM, TOTAL	2210	157
POTASSIUM, TOTAL	1190	470
AMMONIA	570	686
<b>MAJOR ANIONS</b>		
CHLORIDE	150000	87000
BROMIDE	1120	489
SULFATE	400	320
FLUORIDE	0.70	0.98
CARBONATE (ALKALINITY)	<2	<5
<b>OTHER METALS / METALLOIDS</b>		
BARIUM, TOTAL	3.12	2.94
BORON, TOTAL	35.3	28.5
IRON, TOTAL	31.7	44.9
MANGANESE, TOTAL	4.54	1.02
STRONTIUM, TOTAL	1205	577
TITANIUM, TOTAL	25.1	1.98

Table A2: Produced Water Comparisons to USGS Database

		Basin	Ph	Units	Ba	HCO3	Ca	Cl	FeTot	K	Mg	Na
State	Wyoming	<i>Big Horn</i>	8.4	mg/L	0.7	9700	15	166	1	10	8	1540
		<i>Green River</i>	7.0	mg/L	37	1409	1680	9346	32	96	33	4862
		<i>Powder River</i>	7.8	mg/L	15	1463	898	1455	9	24	32	1008
		<i>Wind River</i>	7.9	mg/L	7	4716	9	978	18	71	3	2436
	Illinois	<i>Illinois</i>	7.2	mg/L	4	159	2960	68609	45	144	1118	39158
	Oklahoma	<i>Arkoma</i>	6.2	mg/L	250	317	4777	55728	16	120	1369	27302
	Texas	<i>East Texas</i>	5.5	mg/L	114	131	15449	101438	109	2944	1442	41889
		<i>Gulf Coast</i>	6.1	mg/L	649	305	2290	72925	215	453	320	43539
	Colorado	<i>Raton</i>	8.2	mg/L	1	1076	1102	12	2	3	613	879
		<i>San Juan</i>	8.0	mg/L	2	4255	8447	66	249	27	575	3428
	This Study	Delaware	6.0	mg/L	3.1	2.0	13100	150000	32	1190	2210	57200
		Midland	6.7	mg/L	3	5	1120	87000	45	470	157	38000

Table A3: pHs of Some Solutions used in Sand Column Trials

		PY (mM)	EDTA (mM)	pH	adjusted pH
PRUSSIAN YELLOW TRIALS	NaCl	0	0	6.13	
		1	0	6.02	
		10	0	8.3	
	Del	0	0	6.14	
		1	0	6.38	
		10	0	6.49	
	Mid	0	0	7.34	
		1	0	7.54	
		1.5	0	7.56	
		2	0	7.57	
		3	0	7.59	
		5	0	7.58	
		7	0	7.58	
		10	0	7.6	
	EDTA TRIAL w/o pH adjust	Del	1	0	6.08
1			10	2.64	
1			50	2.36	
1			100	2.38	
1			200	2.415	
EDTA TRIAL w/ pH adjust	Del	1	0	6.33	7.05
		1	5	2.95	7.1
		1	10	2.79	6.95
		1	50	2.61	7.16
		1	100	2.6	7.17
	Mid	1	0	7.28	
		1	1	7.32	
		1	1	7.55	
		1	5	6.03	7.41
		1	10	4.08	7.28
		1	50	3.54	7.29
		1	100	3.49	7.27
		1	100	3.52	7.29

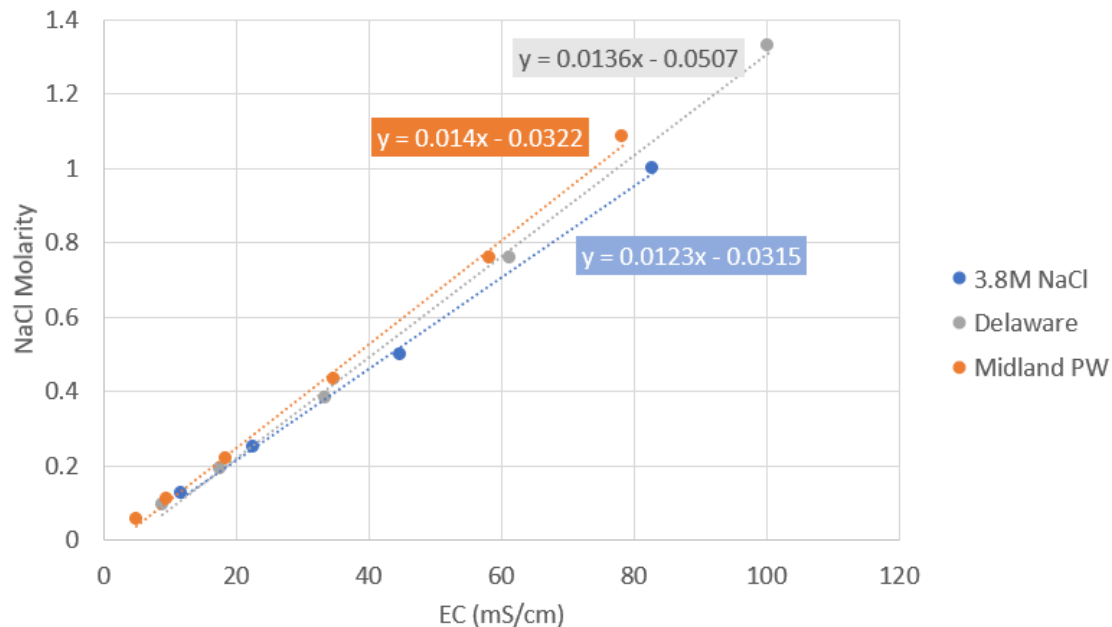


Figure A1: Calibration curves for electroconductivity of brines and corresponding molarities.

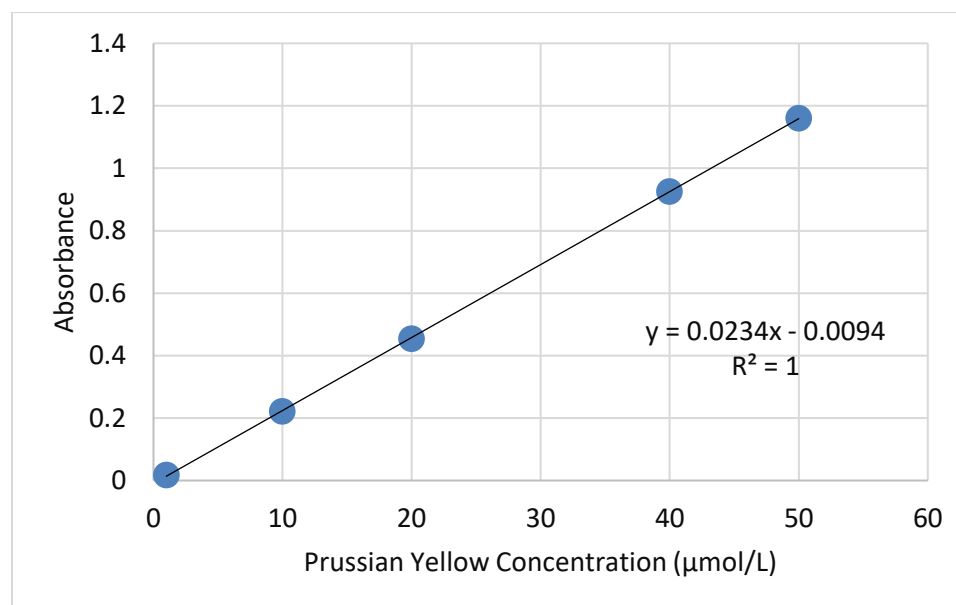


Figure A2: Calibration curve for Prussian yellow concentration and corresponding absorbances.

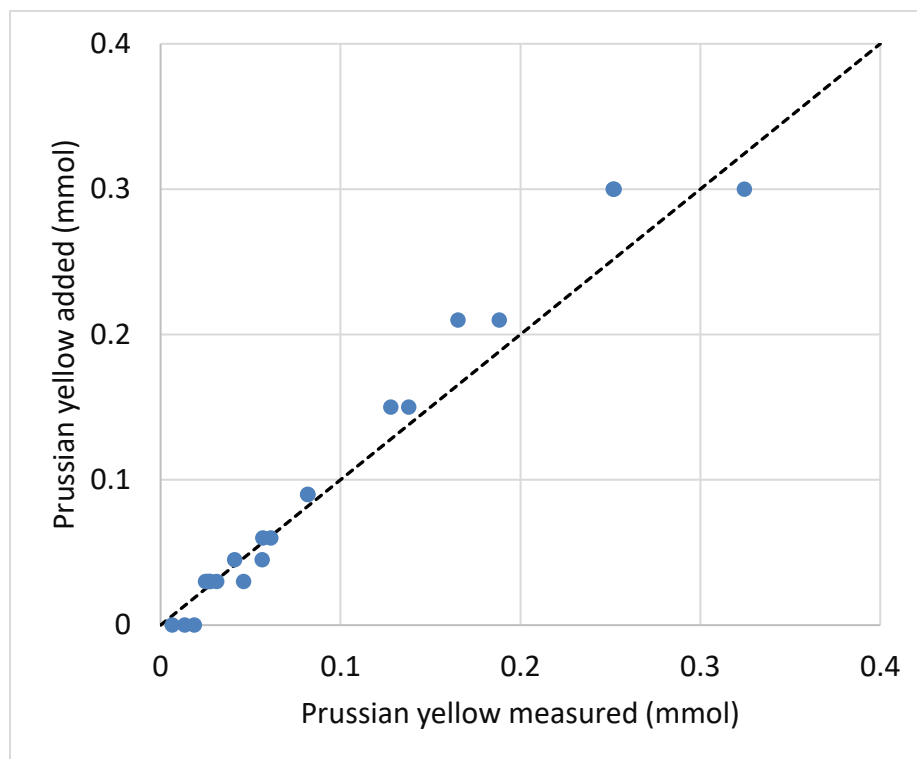


Figure A3: Efficiency of using spectrophotometry to measure Prussian yellow presence in the beakers. Y-axis values are the moles of Prussian yellow added to solution at the beginning of the experiment. X-axis values are the total moles of Prussian yellow found in the surface-scraped salt and remaining sand column after evaporation. X-axis values were determined using spectrophotometry and the calibration curve found in Figure A2

## **Appendix B**

### **SUMMARY OF YEAR 1 WORK WITH BARITE**

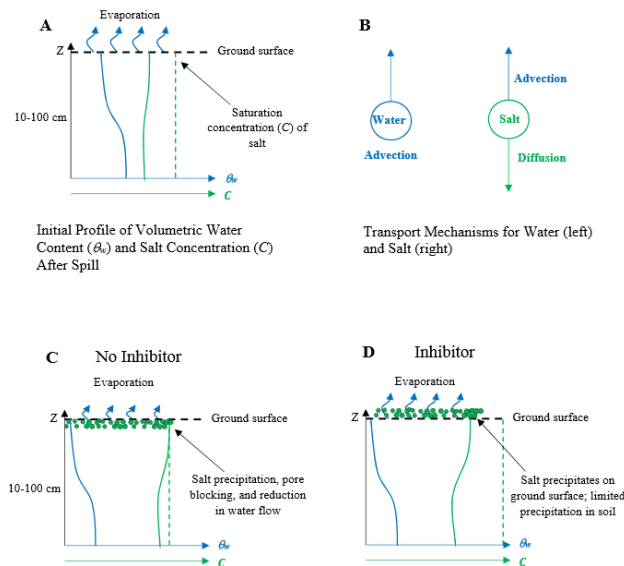
The following is a summary of the first year of work on this project. Initially barite was explored as the salt of concern before focuses were switched towards halite. The knowledge and lessons learned are documented here.

#### **THE PROBLEM**

There is potential for spillage during multiple steps of the hydraulic fracturing process, including during pumping, tank loading, and transport. Most produced waters are highly saline and thus the introduction of high concentrations of ions to the soil profile from accidental spills causes problems. Spills cause soil dispersion and erosion which is often attributed to the replacement of calcium cations in the soil structure by larger hydrated ions such as sodium, which is typically found at high concentrations in produced water. The larger ions cannot flocculate the negatively charged soil particles like calcium, and thus clays may be dispersed leading to pore clogging and loss of infiltration capacity. High salt concentrations also cause death of plants and bacteria that simply are not adapted for such saline environments, and the soil may be deemed infertile.

Current remediation techniques are often costly or invasive. One example is flushing with freshwater, which usually requires significant quantities of water and is more of a salt dilution than removal technique. Another technique is soil removal and replacement, which is costly and further disrupts the soil structure. The addition of calcium to soil to displace the added sodium has also been attempted, but again the salts are not actually removed but flushed into deeper soil and may eventually contaminate groundwater.

In 2016, Daigh and Klaustermeier from North Dakota University published a paper showing that in the presence of ferric hexacyanoferrate (Prussian blue), a known crystallization inhibitor, 29-57% of a sodium chloride “spill” could be removed from the surface of a soil profile by natural evaporation (Klaustermeier et al., 2017). Without the inhibitor, a negligible amount of salt made it to the surface. A diagram to visually explain the technique is shown below. The initial situation after a spill of produced water is illustrated in (A). Salts in the produced water are at high concentrations in soil water, but not sufficiently high to cause precipitation. Natural evaporation at the ground surface drives water movement upward. Salt moves upward with this water, as shown in (B). This transport causes salt concentrations to increase near the soil surface and without a crystallization inhibitor the salts precipitate, fill soil pores, and slow the upward movement of water as shown in (C). When a



(A) Schematic of the soil profile at a brine-contaminated site showing water and salt concentration gradients. (B) Salts are expected to move upwards within the soil along with the advection of water. (C) Clogging of soil pores without inhibitor vs. (D) efflorescence on the soil surface with inhibitor.

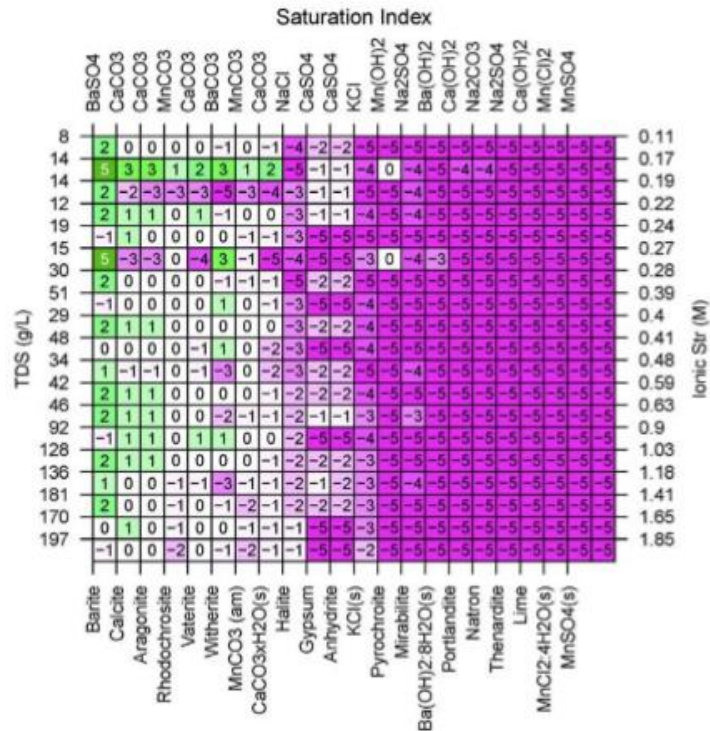
crystallization inhibitor is added to the soil, though, this process is altered. Instead of precipitating in soil pores, salts effloresce on the soil surface where they may be collected and removed from the environment as illustrated in (D).

## KEY FINDINGS

### BARITE

Preliminary speciation calculations using Visual MINTEQ were performed for 19 flowback waters reported in the literature (Haluszczak et al., 2013). This data is displayed in the figure to the

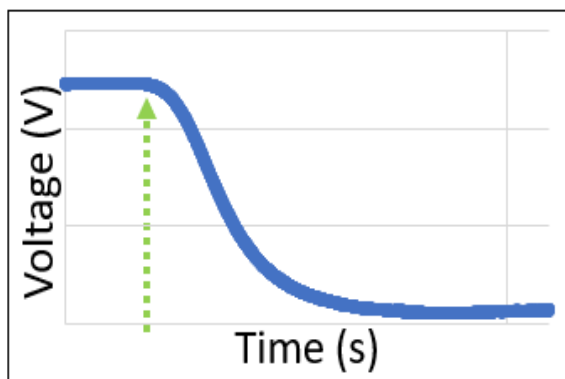
right where each row corresponds to one of the 19 flowback waters, which are ordered by increasing ionic strength shown on the right vertical axis. The left vertical axis reports the total dissolved solids for each flowback water. Each column represents a salt that could potentially form due to the ions present. The numbers and colors in each square correspond to the saturation index for each salt within each water. The saturation index (SI) is a measure to determine when



Heat map of saturation indices of individual salts (columns) in 19 flowback waters (rows). Green is supersaturated and purple is undersaturated. Suggests barite will precipitate

salts are expected to precipitate out of solution. An SI of zero corresponds to equilibrium between dissolved and precipitated states and therefore any SI above zero, shown as green tones, is supersaturated and expected to crystallize. Likewise, an SI below zero, purple tones, is not expected to precipitate. The data suggest that barite ( $\text{BaSO}_4$ ) will be the salt most likely to precipitate first as production waters are evaporated, as it shows the greatest frequency of supersaturation. Due to this, simple barite solutions were investigated first.

The first aspect that had to be determined was how the formation of salt would be quantified. Literature reviews suggested a laser system could be used (Yan et al., 2015). A laser is magnified onto a glass reaction chamber and on the other side of the chamber is a photodiode that records the transmitted light. If the SI for a salt in



*Change in voltage over time as barite crystallization occurs. Green arrow: induction time*

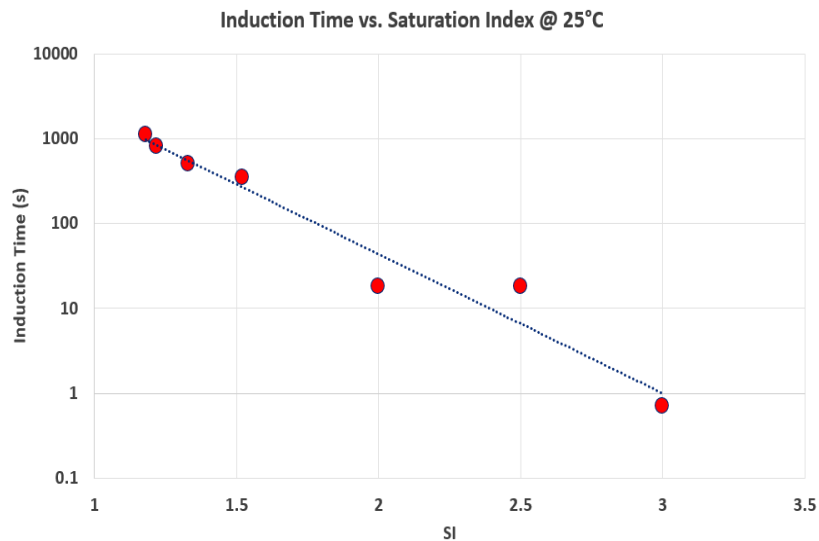
solution exceeds zero, the salt is expected to crystallize in the reaction chamber.

However, this process is not instantaneous and begins to occur at the “induction time,” which is the time elapsed between the establishment of supersaturation and the formation of detectable crystalline phases. In the experimental system, before salts precipitate the voltage read by the

photodiode is at a maximum. As salts begin forming in the reaction chamber, voltage drops as the particles scatter and adsorb light. The timepoint marked by the initial decrease in voltage, signified by the green arrow on the example experimental curve above, is the induction time. In the literature, the addition of crystallization inhibitors increase the induction time. Thus, this setup allowed us to evaluate the utility of

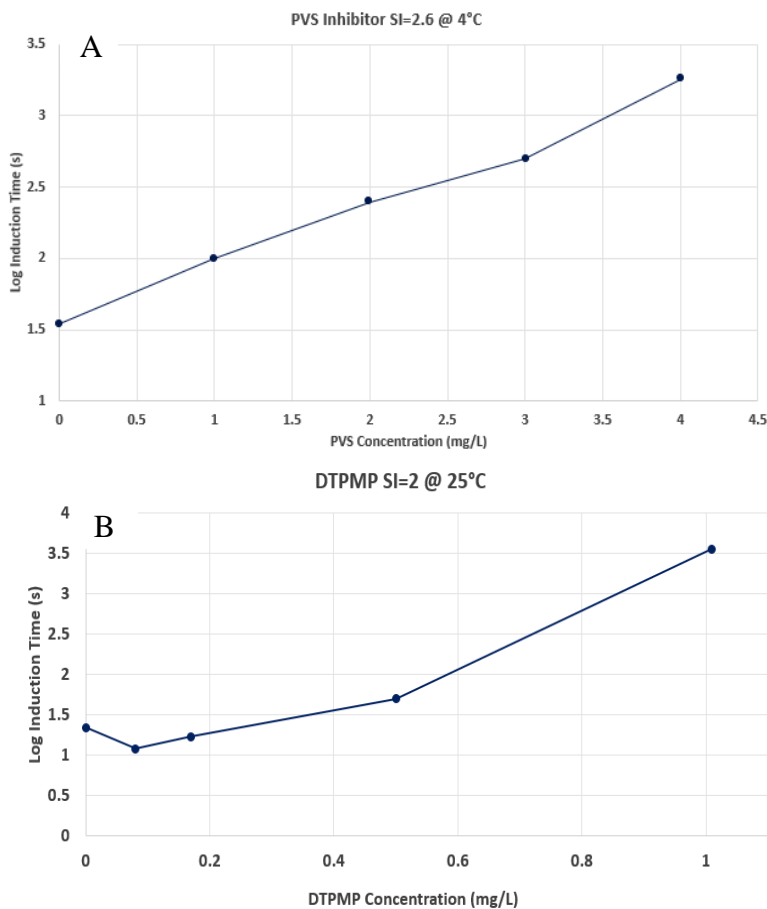
different crystallization inhibitors on the precipitation of salts first from single-salt solutions, e.g., barite, and eventually with produced waters.

This experimental set up made it possible to test the onset of barite crystallization for different conditions, including differing saturation indices (figure below) and the presence or absence of inhibitor (figure on next page). There is a linear relationship between the barite SI and the log induction time. This relationship is logical as the greater the degree of supersaturation (larger SI), the more interactions between ions will occur, and the quicker salts will form.



*Log-linear relationship between barite saturation index and the time until onset of crystallization*

Once the patterns of the onset of crystallization were understood without inhibitor, the addition of inhibitor was explored. Two known barite crystallization inhibitors were tested: diethylenetriamine-penta (methylene phosphonic) acid (DTPMP) and polyvinyl sulfonate (PVS). DTPMP is a monomeric inhibitor with 5 phosphonate groups while PVS is a polymeric inhibitor with one sulfonate group per



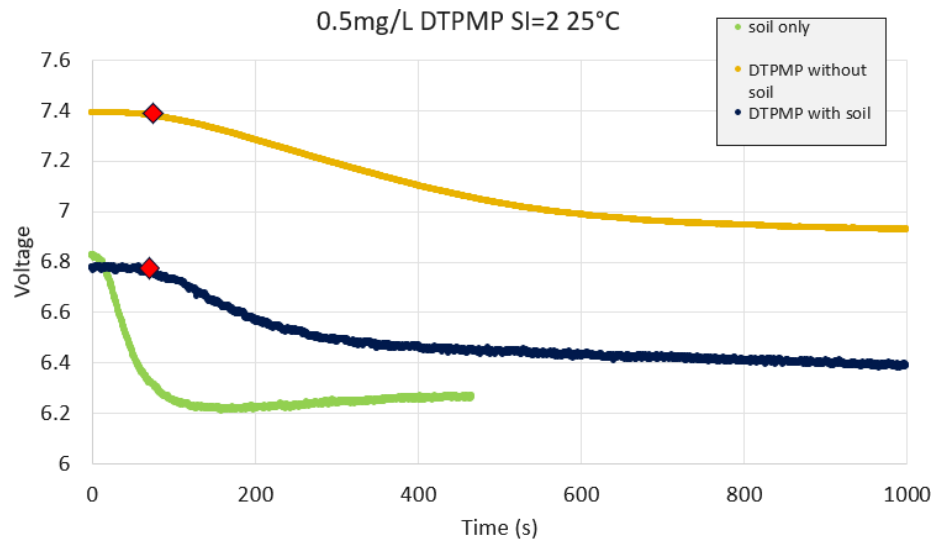
*Effect of concentration of (A) PVS, a sulfonate-based inhibitor, and (B) DTPMP, a phosphonate-based inhibitor, on the time until the onset of barite*

monomer. It has been reported that DTPMP is more efficient than PVS as the phosphonate groups can interact more easily with the barite molecules. This was confirmed by the experimental results (left figure) as the inhibitor concentrations required to lengthen the induction time were smaller for DTPMP than for PVS. The overall observed trend is that as inhibitor concentration increases, the time until the onset of crystallization increases. It is important

to note that since data are reported in log time, only small (mg/L) concentrations are needed to increase induction times 10,000-fold.

In the context of the real-world problem, soil will also play a role in crystallization dynamics. To gain insight into the effects of soil, 2mg/L of soil was added to the system, both with and without DTPMP inhibitor (figure on next page). By comparing the green (soil only) and blue (soil + DTPMP) curves, DTPMP was again observed to increase the induction time (initial voltage drop). Upon comparing the trial with

DTPMP only (yellow) and the trial with both DTPMP and soil (blue), we obtained a new finding that the incorporation of soil does not affect the induction time significantly. This suggests that results from experiments completed without soil will be comparable to those with soil, and that soil-free experiments may be useful for evaluating the efficacy of alternative crystallization inhibitors.



*Voltage curves versus time for the crystallization of barite in the presence of soil (green), DTPMP (yellow), and both DTPMP & soil*

## PRODUCED WATER

ExxonMobil provided samples from two subunits within the Permian basin: the Delaware Basin and the Midland Basin. Subsamples of the produced waters were sent to Alpha Analytical Labs (Westborough, MA) for analysis and their elemental compositions are reported in the table on the following page. The measurements from this analysis were used as input for PHREEQC, a chemical equilibrium speciation modeling program. This program makes use of the Pitzer equations that allow for calculation of aqueous ion activity coefficients in high ionic strength solutions, such as highly saline produced water. PHREEQC was used to estimate the salts that existed as precipitates in the produced water. These predictions are shown as the first bar on the are shown as the first bar on the

*Alpha Analytical lab analysis results of produced water compositions.*

ANALYTE	DELAWARE	MIDLAND
<b>GENERAL PARAMETERS</b>		
pH	6.0	6.7
TOTAL SUSPENDED SOLIDS	100	290
NITROGEN, TOTAL KJELDAHL	618	713
NITROGEN, AMMONIA	570	686
TOTAL ORGANIC NITROGEN	48.0	27.0
PHOSPHORUS, TOTAL	0.605	0.110
<b>MAJOR CATIONS</b>		
SODIUM, TOTAL	57200	38000
CALCIUM, TOTAL	13100	1120
MAGNESIUM, TOTAL	2210	157
POTASSIUM, TOTAL	1190	470
AMMONIA	570	686
<b>MAJOR ANIONS</b>		
CHLORIDE	150000	87000
BROMIDE	1120	489
SULFATE	400	320
FLUORIDE	0.70	0.98
CARBONATE (ALKALINITY)	<2	<5
<b>OTHER METALS / METALLOIDS</b>		
BARIUM, TOTAL	3.12	2.94
BORON, TOTAL	35.3	28.5
IRON, TOTAL	31.7	44.9
MANGANESE, TOTAL	4.54	1.02
STRONTIUM, TOTAL	1205	577
TITANIUM, TOTAL	25.1	1.98

evaporation on solution chemistry and salt precipitation. PHREEQC was applied in this mode, and these results are also shown in section a and b of the figure on the next page.

left (0% evaporation) in the figure on the next page (section a and b).

PHREEQC indicates that barite will be one of the first salts to precipitate (navy bar), as was initially suspected. However, celestite ( $\text{SrSO}_4$ , yellow bar) also precipitates immediately and in greater volume than barite. This was a new finding which holds true for both basins. Fortunately, since both salts are sulfate based, the same inhibitors are reported to be efficient for both.

PHREEQC can also describe the effect of water

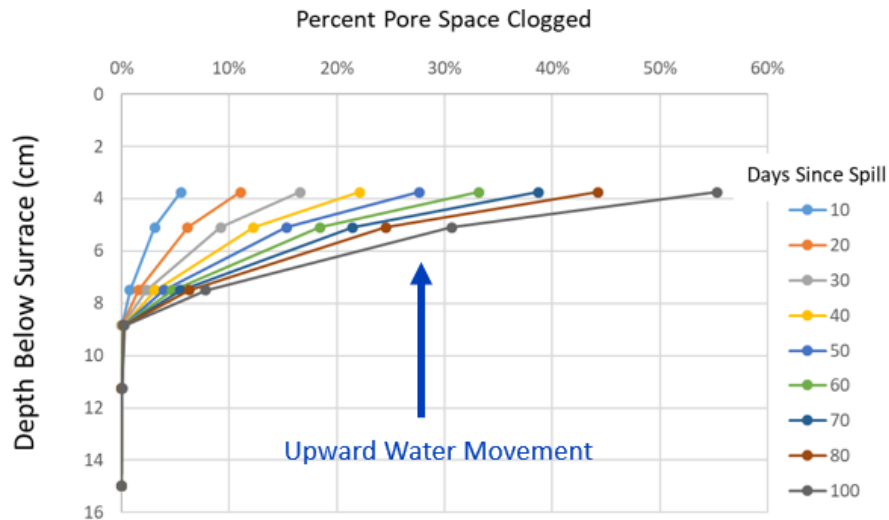


*PHREEQC predictions of relative volumes of each salt crystallized as percent evaporation increases for the a) Delaware and b) Midland produced waters. Individual volumes (cm<sup>3</sup>/L) of each salt are also reported for the c) Delaware and d) Midland basin, with darker green being higher volumes.*

PHREEQC predicts that 41% and 67% water evaporation is required, respectively, for the Delaware and Midland basins to reach the solubility limit of halite (NaCl, grey bars). It takes longer for the Midland basin to crystallize halite due to much lower initial sodium and chloride concentrations. The most surprising finding was that once halite begins to precipitate it does so in much greater volume than the previously precipitated barite and celestite. Thus, halite is likely to play a more important role than barite and celestite in soil pore clogging. The heat maps of the volume of each salt precipitated at each evaporation percentage are shown in sections c and d of the figure above. These maps highlight the differences in precipitated volume for each salt: white cells indicate no salt precipitation, while light to dark green shading indicates increasing volume of precipitated salts. If we examine the Delaware basin

after 75% evaporation, for example, 211 cm<sup>3</sup>/L of halite versus only 1 cm<sup>3</sup>/L of celestite is expected to precipitate.

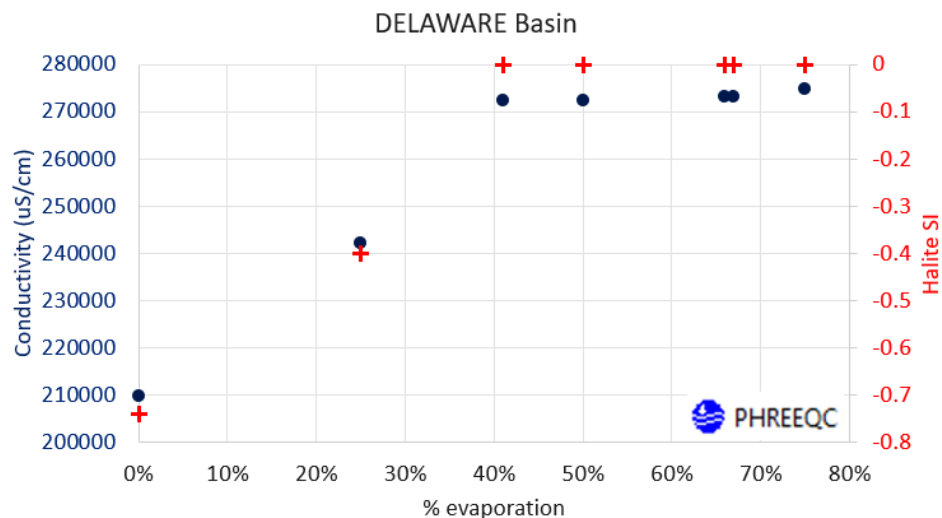
Very preliminary calculations were performed to determine the effect that these crystallized salt volumes would have on the clogging of soil pores after an accidental spill of produced water. The graph below is for a spill of produced water from the Delaware Basin in west Texas and illustrates the predicted vertical profile of pore clogging after a spill on day 0. Typical rates of evapotranspiration were assumed for west Texas, which drives soil water to the ground surface. As the water evaporates, salts precipitate and fill soil pores. The graph suggests that 100 days after a spill, the soil near the surface would be about 55% clogged and over 95% of that would be due to the crystallization of halite.



*Soil clogging predicted for natural evaporation of a Delaware Basin produced water spill from a soil profile over time*

The PHREEQC model was also used to predict the change in electrical conductivity of the produced water solutions as they undergo evaporation, and the results are shown on the next page. Superimposed on this plot is the halite SI. As the halite SI increases from undersaturated towards SI = 0, the saturation point, the

conductivity also linearly increases. Once  $SI = 0$ , it plateaus and remains at zero as any further evaporation would only cause more crystallization: the solution does not become supersaturated. The conductivity also remains steady once  $SI = 0$ . The sharp change in slope of electrical conductivity at  $SI = 0$  suggests that electrical conductivity can be used to detect the beginning of halite crystallization. Electrical conductivity can be measured using specialized conductivity probes for measuring conductivity in the very saline solutions. Based on these findings from PHREEQC simulations of the produced waters, the focus of the investigation changed from barite to halite as the most important salt causing pore clogging, and from lasers to electrical conductivity measurements for assessing the onset of crystallization.

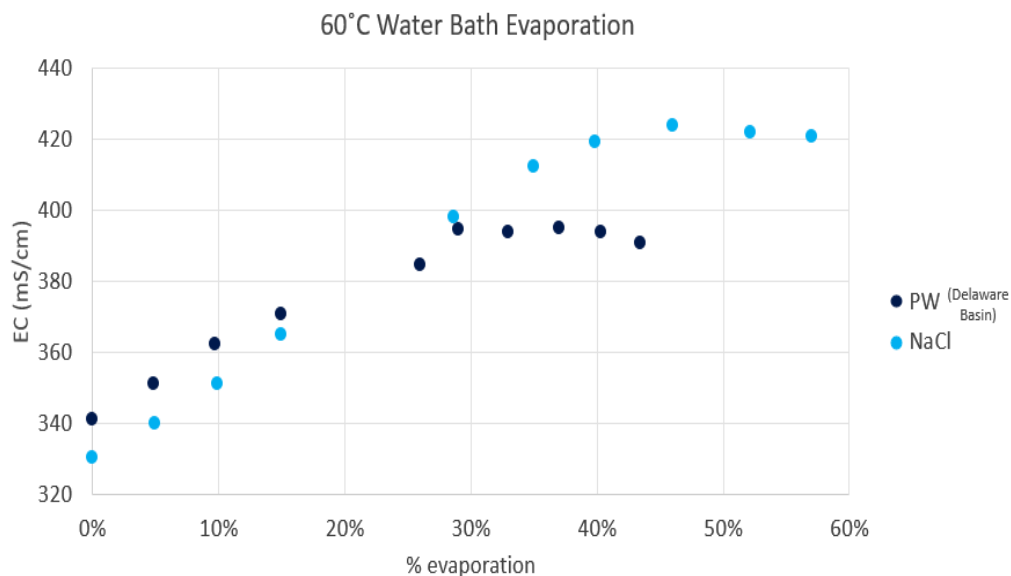


PHREEQC predictions of chemical changes with evaporation of Delaware Basin produced water. Conductivity (navy) and halite saturation index (red).

## HALITE

To assess the accuracy of PHREEQC simulations in both produced water and halite solutions, evaporation experiments were conducted with these solutions in batch reaction vessels without soil and with an electrical conductivity probe capable of

measuring conductivity at high salt concentrations. The results are shown in the figure below and for both produced water and halite solutions the electrical conductivity increased as evaporation progressed and then remained constant with time (and degree of evaporation) once salt precipitation was visually observed. Crystallization of salt in the Delaware Basin produced water occurred slightly earlier than expected, at 30% evaporation rather than 40% evaporation as predicted by PHREEQC. In the simpler solution containing only halite, salt precipitated at approximately 40% evaporation, consistent with the PHREEQC prediction (not shown) which is also when the electrical conductivity ceased to change with evaporation.

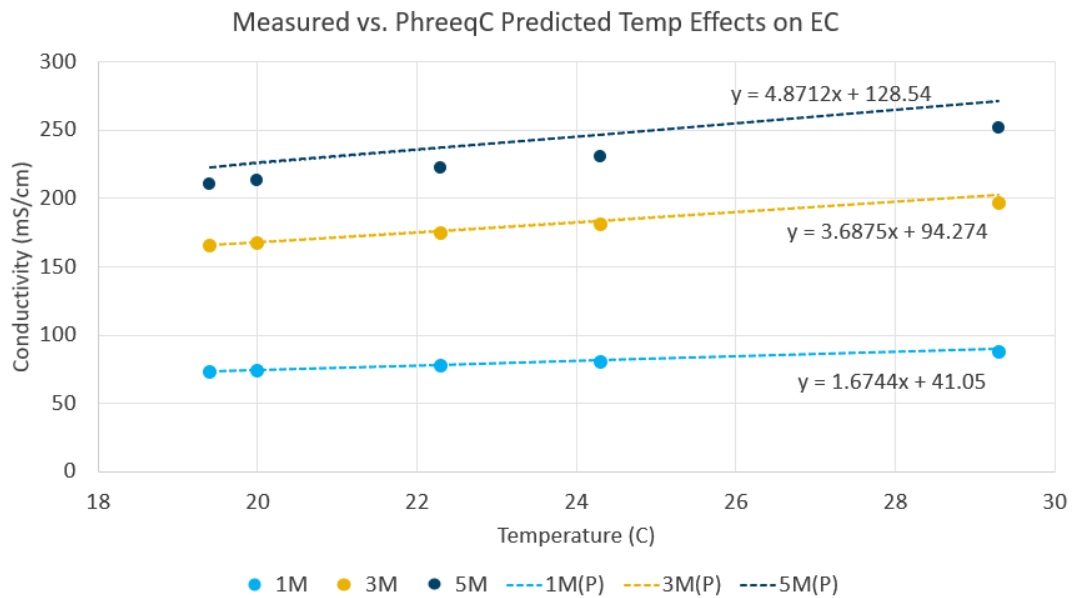


*Experimental results of conductivity patterns during the evaporation of Delaware Basin produced water (navy) and a simple halite solution (aqua).*

These experiments validated the PHREEQC predictions for halite and demonstrated that electrical conductivity could be used to determine the onsite of halite precipitation. While the agreement between PHREEQC predictions and produced water data was not as good as for the pure halite solution, the model predictions agreed sufficiently well with data that PHREEQC may be used to guide

selection of inhibitors and to assist in the design and interpretation of experiments. Electrical conductivity has also been shown as useful measurement to track solution chemistry and may be used in laboratory soil column experiments and in the field to monitor the saturation index of halite, the most prevalent salt in the Delaware and Midland basin produced waters.

Additional experiments were conducted with the electrical conductivity probe to assess its internal temperature correction, since evaporation experiments that mimic natural evaporation in the field will cool solutions. The effect of temperature on electrical conductivity increases with salt concentrations or molarity (M), as shown on the next page. This is important to note as temperatures at actual spill sites will vary from state to state and with season, and therefore temperature will need to be incorporated into monitoring programs if electrical conductivity is used to track changes in solution chemistry. It was also shown that the PHREEQC predictions (P, dashed lines) match experimental data better at lower molarities, while PHREEQC overpredicts electrical conductivity at higher concentrations. The systematic difference between PHREEQC predictions and electrical conductivity measurements in solutions with high molarities will be important to consider as these high ranges will be seen in the produced waters. The Delaware Basin, prior to any evaporation, has a chlorine molarity of 4.2 mol/L, corresponding to a PHREEQC conductivity of 210 mS/cm, about the conductivity where we begin to see variation between PHREEQC and the probe. The Midland basin begins with a lower 2.5 mol/L chlorine molarity and a conductivity of 152 mS/cm which is within the range where PHREEQC and the probe are in good agreement, however after about 37% evaporation, the conductivity of the Midland would rise to about 210 mS/cm, near the range where systematic differences are observed.



*Effects of temperature on conductivity for 1 mol/L (M), 3M, and 5M NaCl solutions. Data points are experimentally measured conductivities and dashed lines are PHREEQC predicted conductivities*

## SUMMARY

The focus of the research has shifted over the past year from barite to halite, but at each step new insights have been found as progress is made towards finding a solution. For the initial research surrounding barite, it was found that a laser system can be successfully implemented to quantify crystallization. Using this system it was possible to confirm that at higher salt concentrations, crystallization will occur much faster. However, the presence of small amounts of inhibitor can delay the onset of crystallization, with phosphonate-based inhibitors (DTPMP) showing stronger efficiency than sulfonate-based inhibitors (PVS). It was concluded that although the sulfate-based salts, barite and celestite, will precipitate soonest, halite (NaCl) holds the

most potential for soil pore clogging once its solubility limit is reached. Sodium and chloride are present in much higher abundances in the produced waters than barium, strontium, and sulfate and thus halite forms in much larger volumes. It will, however, take about 41% and 67% evaporation, respectively, for the Delaware and Midland basin produced waters to reach halite's solubility limit for precipitation to occur. The characterization of the individual basins has provided insight into the dramatic compositional variation, dependent upon site location. This variation will need to be incorporated into determining effective inhibitor concentrations based on the chemistry of each site. Another factor that has been proven significant is temperature, which has been found to play a key role in both conductivity measurements and crystallization kinetics.

As the research continues, a focus will be placed on the use of conductivity as a measure of the onset of halite crystallization. This system of quantification will be implemented into simple solutions of halite, as well as in the produced waters to investigate the effects of halite inhibitors, such as prussian blue in batch evaporation trials. The inhibitors found most effective in increasing induction time and decreasing crystal size will then be tested in soil column experiments. The soils used will be chosen to reflect the soils of the basin locations. Spectroscopic and chromatographic techniques, such as XRD and XEDS, will be used to confirm the identity of the salts forming during evaporative trials. Along with this a computational model to interpret

the data and describe the transport of water, dissolved ions, and inhibitor within the soil profile will be developed. This model will serve as a guide for future research, allowing underlying mechanisms to be better understood and manipulated for solution development.

#### **REFERENCES**

Haluszczak LO, Rose AW, Kump LR. Geochemical evaluation of flowback brine from Marcellus gas wells in Pennsylvania, USA. *Appl Geochemistry* 2013;28:55–61. <https://doi.org/10.1016/j.apgeochem.2012.10.002>.

Klaustermeier AW, Daigh ALM, Limb RF, Sedivec K. Crystallization inhibitors and their remediation potential on brine-contaminated soils. *Vadose Zo J* 2017;16. <https://doi.org/10.2136/vzj2016.10.0095>.

Yan C, Kan AT, Zhang F, Liu Y, Tomson RC, Tomson MB. Systematic study of barite nucleation and inhibition with various polymeric scale inhibitors by novel laser apparatus. *SPE J* 2015;20:642–51. <https://doi.org/10.2118/169787-PA>.